Atmos. Chem. Phys. Discuss., 11, 20575–20629, 2011
www.atmos-chem-phys-discuss.net/11/20575/2011/
doi:10.5194/acpd-11-20575-2011

Atmospheric Chemistry and Physics Discussions

Aerosols in the CALIOPE air quality modelling system: validation and analysis of PM levels, optical depths and chemical composition over Europe

S. Basart[1], M. T. Pay[1,2], O. Jorba[1], C. Pérez[3], P. Jiménez-Guerrero[4], M. Schulz[5], and J. M. Baldasano[1,2]

[1]Earth Sciences Department, Barcelona Supercomputing Center-Centro Nacional de Supercomputación, BSC-CNS, Barcelona, Spain
[2]Environmental Modelling Laboratory, Technical University of Catalonia, Barcelona, Spain
[3]Earth Institute at Columbia University, NASA Goddard Institute for Space Studies and International Research Institute for Climate and Society, New York, USA
[4]Physics of the Earth, Department of Physics, University of Murcia, Spain
[5]Norwegian Meteorological Institute, Oslo, Norway

Received: 29 April 2011 – Accepted: 13 July 2011 – Published: 19 July 2011

Correspondence to: J. M. Baldasano (jose.baldasano@bsc.es)

Published by Copernicus Publications on behalf of the European Geosciences Union.

Abstract

The CALIOPE high-resolution air quality modelling system is developed and applied to Europe (12 km × 12 km, 1 h). The modelled daily to seasonal aerosol variability over Europe in 2004 have been evaluated and analysed. The aerosols are estimated from two models, CMAQv4.5 (AERO4) and BSC-DREAM8b. CMAQv4.5 calculates biogenic, anthropogenic and sea salt aerosol and BSC-DREAM8b provides the natural mineral dust contribution from North African deserts. For the evaluation, we use daily PM10/PM2.5 and chemical composition data from 54 stations of the EMEP/CREATE network and coarse and fine aerosol optical depth (AOD) data from 35 stations of the AERONET sun photometer network. The model achieves daily PM10 and PM2.5 correlations of 0.57 and 0.47, respectively, and total, coarse and fine AOD correlations of 0.51, 0.63, and 0.53, respectively. The higher correlations of the PM10 and the coarse mode AOD are largely due to the accurate representation of the African dust influence in the forecasting system. Overall PM and AOD levels are underestimated. The evaluation of the chemical composition highlights underestimations of the modelled fine fractions particularly for carbonaceous matter (EC and OC) and secondary inorganic aerosols (SIA; i.e. nitrates, sulphates and ammonium). The scores of the bulk parameters are significantly improved after applying a simple model bias correction based on the chemical composition observations. SIA are dominant in the fine fractions representing up to 80 % of the aerosol budget in latitudes beyond 40° N. The highest aerosol concentrations are found over the industrialized and populated areas of the Po Valley and the Benelux regions. High values in southern Europe are linked to the transport of coarse particles from the Sahara desert which contributes up to 40 % of the total aerosol mass. Close to the surface, maxima dust seasonal concentrations (>30 $\mu g\,m^{-3}$) are found between spring and early autumn. We estimate that desert dust causes daily exceedances of the PM10 European air quality threshold (50 $\mu g\,m^{-3}$) in large areas south of 45° N reaching up to more than 75 days per year in the southernmost regions.

ACPD

11, 20575–20629, 2011

1 Introduction

Atmospheric aerosols or particulate matter (PM) are highly inhomogeneous and variable in space and time due to the variety of their sources and their fast removal from the atmosphere (from days to weeks). Aerosols contribute to adverse human health effects (WHO, 2005), including increased morbidity and mortality arising from altered respiratory and cardiovascular function (Pope et al., 2009; Medina et al., 2009) and have a significant, yet uncertain effect on climate from regional to global scales (IPCC, 2007). To understand the wide-ranging effects of aerosols, it is important to characterize them with high spatial and temporal resolution.

The *European Union (EU) directive on ambient air quality and cleaner air* which entered into force in June 2008 and may have been transposed into the national legislation of each Member State by June 2010 (European Commission, 2008), introduces daily and annual PM10 limit values of 50 $\mu g\,m^{-3}$ and 40 $\mu g\,m^{-3}$, respectively, from year 2010. Also this directive introduces a PM2.5 annual limit value of 25 $\mu g\,m^{-3}$ to be assumed from year 2015. In this regard, the objectives proposed by the EU are usually less well attained in southern Europe than in northern countries (Yttry and Aas, 2006). Reports from countries around the Mediterranean Basin and Eastern Europe show high levels of atmospheric PM compared to Northern and some central European regions (Querol et al., 2009). Both anthropogenic (transport sector, industrial processes, power generation and biomass burning, among others) and natural (African dust, resuspension, sea spray, forest fires, primary biological particles and biogenic secondary organic compounds) emissions, as well as orographic and climatic factors contribute to those enhanced PM levels. When PM10 values are exceeded due to natural events (such as desert dust outbreaks or volcano eruptions), Member States shall inform the Commission, providing the necessary justification to demonstrate that such exceedances are due to natural events.

Air quality models are useful to understand the dynamics and transport of pollutants and manage air quality. In recent years a number of experimental and operational

ACPD
11, 20575–20629, 2011

air quality forecast systems have been developed around the world. Nowadays, in Europe, 23 modelling systems routinely simulate the air quality over Europe, 7 systems also operate in forecasting mode (Menut and Bessagnet, 2010): PREV'AIR, EURAD, EMEP-CWF, MATCH, MOCAGE, CHIMERE, and CALIOPE.

In the frame of the CALIOPE system (Baldasano et al., 2008a; http://www.bsc.es/caliope), the Barcelona Supercomputing Center-Centro Nacional de Supercomputación (BSC-CNS) operates an air quality forecasting system for Spain (at 4 km × 4 km horizontal resolution) and Europe (at 12 km × 12 km horizontal resolution) with WRF-ARW/HERMES-EMEP/CMAQ and desert dust forecasts with BSC-DREAM8b (Nickovic et al., 2001; Pérez et al., 2006a, b). In contrast to many other forecasting systems, CALIOPE includes a non-climatic representation of African dust transport. The forecasts are evaluated on a daily basis against ground-based and satellite observations to establish confidence of the modelling system predictions among users, identify problems and routinely improve the system (Baldasano et al., 2010).

Pay et al. (2010) presented a full year evaluation of the CALIOPE system for the European domain for gaseous pollutants (O_3, NO_2 and SO_2) and PM levels (PM10 and PM2.5) against EMEP ground-based measurements. The study shows that the skill scores of the system lie within the range of most European models and that while the dynamics of PM2.5 and PM10 are rather well reproduced, concentrations remain systematically underestimated about a factor of 2 on average.

The main objective of the present work is to complement the results of the PM evaluation presented in Pay et al. (2010) by (1) providing a detailed quantitative assessment of the capabilities of the CALIOPE system to simulate the daily aerosol distribution over Europe for year 2004 in terms of PM levels, aerosol optical depth (AOD) and chemical composition; (2) understanding the underestimation of the PM mass; (3) estimating and analysing the spatial and seasonal distribution of the different aerosol fractions over Europe based on the model results and observations; and (4) estimating the exceedances of the EU limits due to natural desert dust.

ACPD
11, 20575–20629, 2011

The manuscript is organized as follows. Section 2 describes the CALIOPE system and the observational datasets used for the model evaluation. In Sect. 3 we use aerosol chemical composition from EMEP/CREATE and AOD from the AERONET network to identify the origin of the discrepancies in PM levels. The evaluation of the AOD is particularly useful for validating and analysing the capabilities of the modelling system to reproduce long-range transport of desert dust from North Africa. In Sect. 4 we estimate and analyse the spatial and seasonal distribution of the different natural and anthropogenic aerosol fractions over Europe applying a simple bias correction to the model based on the results of the evaluation. African dust transport and its contribution over Europe are analysed in detail. Finally, Sect. 5 summarizes the findings of the study.

2 Methods

2.1 Description of the CALIOPE system

CALIOPE is a state-of-the-art air quality modelling system that integrates an emission-processing model (HERMES-EMEP), a meteorological model (WRF-ARW), a chemical transport model (CMAQ) and a mineral dust model (BSC-DREAM8b; Pérez et al., 2006a, b). Thus, the aerosols are estimated from CMAQ and BSC-DREAM8b, and they are described in detail in the next sections. The configuration used in the present work is described in Pay et al. (2010). As CALIOPE is a fundamental model system the authors wish to stress that neither correction factors nor any adjusting model parameterization have been applied to the model output or the original model codes used in the model evaluation.

2.1.1 Photochemical model: CMAQ

The Models-3 Community Multiscale Air Quality Modeling system (CMAQ; Byun and Ching, 1999; Binkowski, 1999; Byun and Schere, 2006) is used to study the behaviour

ACPD
11, 20575–20629, 2011

of air pollutants from regional to local scales. CMAQ version 4.5, used in this study, has been extensively evaluated under various conditions and locations (Jiménez et al., 2003; Roy et al., 2007; Wyat Appel et al., 2007, 2008). Following the criteria of Jiménez et al. (2003) the Carbon Bond IV chemical mechanism is applied (CBM-IV, Gery et al., 1989). The production of sea salt aerosol (SSA) is implemented as a function of wind speed and relative humidity (Gong, 2003; Zhang et al., 2005) through the AERO4 aerosol module. The AERO4 module distinguishes among different chemical aerosol components namely nitrate, sulphate, ammonium, elemental carbon and organic carbon with three subcomponents (primary, secondary anthropogenic and secondary biogenic), soil, sodium, and chlorine. Unspecified anthropogenic aerosols and aerosol water are additionally kept as separate components. Unspecified aerosols consists of the non-carbon atoms associated with organic carbon as well as particulate matter emissions that are not explicitly speciated in HERMES-EMEP emission model, which includes traces elements, primary $NH4^+$ and other unidentified mass in the speciation profiles (Wyat Appel et al., 2007). Aerosols are represented by three size modes (Aitken, accumulation and coarse mode), each of them assumed to have a lognormal distribution (Binkowski and Roselle, 2003). Secondary inorganic aerosols (SIA) are generated by nucleation processes from their precursors to form nitrate, ammonium and sulphate aerosols. Secondary organic aerosol (SOA) can be formed from aromatics (anthropogenic organic aerosols) and terpenes (biogenic organic aerosols, Schell et al., 2001). The aerosol microphysical description is based on a modal aerosol model (Binkowski and Roselle, 2003) using the ISORROPIA thermodynamic equilibrium model (Nenes et al., 1998). For a more complete description of the processes implemented in CMAQ, the reader is referred to Byun and Schere (2006).

AOD (at 550 nm) from CMAQ outputs is calculated using a simple approach described by Malm et al. (1994) and Binkowski and Rosselle (2003). The method is known as the "reconstructed mass-extinction method". The extinction coefficient (β_{ext}), which is a function of wavelength (λ), is a sum of the attenuation by scattering (β_s) and absorption (β_a). The model-predicted AOD is calculated by summing the product of

ACPD
11, 20575–20629, 2011

the extinction and layer thickness (ΔZ_i) over the number of layers (N) in the column:

$$\mathrm{AOD} = \sum_{i=1}^{N} (\beta_s + \beta_a)_i \Delta Z_i \quad (1)$$

We estimate the model-predicted $\beta_{ext}=\beta_s+\beta_a$ using this semi-empirical approach for extinction calculation which depends on aerosol mass and humidity as follows:

$$\beta_s = 0.003 f(\mathrm{HR}) \left\{ [\mathrm{NH_4^+}] + [\mathrm{SO_4^-}] + [\mathrm{NO_3^-}] \right\} + 0.004[\mathrm{OM}] + 0.001 [\mathrm{PM_{fine}}] + 0.0006 [\mathrm{PM_{coarse}}]$$

$$\beta_a = 0.01 \cdot [\mathrm{EC}] \quad (2)$$

where the brackets in the above equations indicate mass concentration in mg m^{-3} and all coefficients in the equation represent the specific extinction cross section at 550 nm (in m^2 mg^{-1}). When implementing the above equation, the term in brackets is determined by adding ammonium mass (NH_4^+) plus sulphate mass (SO_4^{2-}) plus nitrate mass (NO_3^-). Organic mass (OM) is taken as the sum of all organic species. Light absorbing carbon is elemental carbon (EC). PM_{fine} mass is taken as the unspeciated portion of PM2.5 and the fine fraction of sodium (Na^+) and chloride (Cl^-), and the PM_{coarse} mass represents all coarse mode aerosols that includes the unspeciated portion of PM10 and the coarse fraction of sodium (Na^+) and chloride (Cl^-). The mass concentration for each of these species is directly obtained from CMAQ. The relative humidity correction factor, f(RH), takes into account that the growth and phase change of hygroscopic particles affect their light-scattering effiency (Malm et al., 1994). f(RH) is parameterized from data published by Tang et al. (1981) as a function of the relative humidity from the WRF-ARW meteorological model and it varies between 1 (at low RH) and 21 (at RH = 99 %).

2.1.2 Mineral dust model: BSC-DREAM8b

The Dust REgional Atmospheric Model (DREAM; Nickovic et al., 2001) was designed to simulate and/or predict the atmospheric cycle of mineral dust. The updated model

ACPD
11, 20575–20629, 2011

version BSC-DREAM8b used here is described in Pérez et al. (2006a, b). It includes an 8-bins size distribution within the 0.1–10 µm radius range according to Tegen and Lacis (1996). In this updated version dust radiation interactions are included.

The BSC-DREAM8b model has demonstrated its capabilities in a number of validation studies performed so far (e.g. Pérez et al., 2006a; Amiridis et al., 2009; Papanastasiou et al., 2010) using data from observation networks such as the European Lidar Network EARLINET, the AERONET/PHOTONS sun-photometer network, satellite and ground-level PM levels. Such validations outline the good skills of the model concerning both the horizontal and vertical extent of the dust plume in Europe and the Mediterranean Basin. Additionally, the model has been validated and tested against measurements at source regions for SAMUM-I (Haustein et al., 2009) and BODEX campaigns (Todd et al., 2008).

In BSC-DREAM8b, the AOD is calculated from the column mass loading by:

$$\mathrm{AOD}(\lambda) = \sum_{1}^{8} \mathrm{AOD}_k(\lambda) = \sum_{1}^{8} \frac{3}{4\rho_k r_k} M_k Q_{\mathrm{ext}}(\lambda)_k \quad (3)$$

where for each size bin k: ρ_k is the particle mass density, r_k is the effective radius, M_k is the column mass loading and $Q_{\mathrm{ext}}\ (\lambda)_k$ is the extinction efficiency factor which is calculated using Mie scattering theory.

2.2 Simulation

The CALIOPE system is run on a regional scale (12 km × 12 km in space) to model the European domain (see Fig. 1). The simulation consists of 366 daily runs (1h in time) to simulate the entire year of 2004.

Emissions used for the European domain are derived from the 2004 annual EMEP emission database (EMEP, 2007) and processed by High-Elective Resolution Modeling Emission System (HERMES, see Baldasano et al., 2008b) in order to provide a comprehensive description of the emissions to the air quality model. Disaggregation of EMEP (50 km resolution) data is performed in space (12 km × 12 km) and time (1 h).

ACPD
11, 20575–20629, 2011

The Final Analyses of the National Centers of Environmental Prediction (FNL/NCEP; at 1° × 1°) at 12 UTC are used as initial conditions and boundary conditions at intervals of 6 h. WRF-ARW (version v3.0.1.1) is configured with a grid of 479 × 399 points and 38σ vertical levels (11 characterizing the PBL). The model top is defined at 50 hPa to resolve properly the troposphere-stratosphere exchanges. The CMAQ horizontal grid resolution corresponds to that of WRF-ARW. Its vertical structure was obtained by a collapse from the 38 WRF-ARW layers to a total of 15 layers steadily increasing from the surface up to 50 hPa with a stronger concentration within the PBL. CMAQ boundary conditions are based on the global climate chemistry model LMDz-INCA2 (Piot et al., 2008; Szopa et al., 2009).

The initial state of dust concentration in the BSC-DREAM8b model is defined by the 24-h forecast from the previous-day model run. The FNL/NCEP (at 1° × 1°) at 0 UTC are used as initial conditions and boundary conditions at intervals of 6 h. The resolution is set to 1/3° in the horizontal and to 24 layers extending up to approximately 15 km in the vertical. The domain of simulation covers northern Africa, the Mediterranean Sea, southern Europe and Middle East. An offline coupling is applied to the calculated concentrations of particulate matter over the European domain from CMAQ outputs (Jiménez-Guerrero et al., 2008).

2.3 Observations

2.3.1 Surface PM and chemical composition from EMEP/CREATE Networks

For the evaluation of PM2.5 and PM10, we have used the same observational dataset included in the analysis of Pay et al. (2010). In this study, model output for PM concentrations are compared with ground-based measurements from the European Monitoring and Evaluation Programme (EMEP) monitoring network for the year 2004. EMEP stations are located at a minimum distance of approximately 10 km from large emission sources (Larssen et al., 1999). EMEP stations are assumed to be representative of regional background concentrations (Torseth and Hov, 2003). A total of 16 and 25

ACPD
11, 20575–20629, 2011

stations for PM2.5 and PM10 respectively have been used to evaluate the model predictions. Details on the location of the EMEP stations used for this comparison as well an accurate analysis of the results can be found in Pay et al. (2010).

Aerosol modelled concentrations for chemical species are compared with ground-based measurements provided by EMEP and the FP5/GMES project CREATE at 54 rural background stations. The uncertainty of aerosol mass measurements strongly depends on the method and chemical composition of the collected aerosol. Usually the collected filters are weighted at 50 % relative humidity (Tsyro, 2005). Error sources which lead to a bias are potential losses of semivolatile compounds (particularly ammonium nitrate and carbonaceous aerosols) from the filters at temperatures higher than 20 °C. Inorganic species may be accurately measured with an uncertainty of about ±10 % for major species (Putaud et al., 2004). In this context, European legislation (2008/50/EC) establishes that measurement groups have to demonstrate that the uncertainty of PM10 and PM2.5 meets the quality objective of 25 %. However legislation does not establish any quality objective for uncertainty of chemical species yet. The inorganic chemical components collected within CREATE are measured by ion chromatography in which the error is usually within 10 % (Putaud et al., 2000).

In the present work, measured aerosol surface concentrations and aerosol mass are available on a daily and annual basis. The main characteristics and location of these EMEP/CREATE stations are described in Table A1 and their locations are displayed in Fig. 1. The CALIOPE system is evaluated at 54 stations: 53 including sulphate (SO_4^{2-}), 27 nitrate (NO_3^-), 15 ammonium (NH_4^+), 9 sodium (Na^+), 5 chloride (Cl^-) and 2 carbonaceous matter (EC and OC). The measurements are well documented and available on the EMEP web page (http://www.emep.int).

2.3.2 Aerosol optical depth from AERONET Network

The optical properties of the aerosol in the entire atmospheric column are routinely observed within the Aerosol Robotic Network (AERONET, Holben et al., 1998; Smirnov et al., 2000). The network imposes standardization of instruments, calibration, processing

ACPD
11, 20575–20629, 2011

and distribution.

Sun photometer measurements of the direct (collimated) solar radiation provide information to calculate the columnar AOD. The typical uncertainty in the direct-sun AOD measurements ranges from 0.01 to 0.02 with higher errors in the ultraviolet spectral range (Dubovik et al., 2000). Additionally, direct-sun AOD processing now includes the Spectral Deconvolution Algorithm (SDA) retrievals (O'Neill et al., 2003). The SDA algorithm yields *fine* (sub-micron) and *coarse* (super-micron) AOD at a standard wavelength of 500 nm from which the fraction of fine mode (FMF) to total AOD can be computed obtaining the fine and coarse fraction of the total AOD (AOD_{fine} and AOD_{coarse}, respectively). The amplitude of the errors of these derived parameters varies as the inverse of the total AOD. There are, in addition to measuremental errors in AOD errors due to the uncertainty in the assumed values of the spectral curvature in each mode (O'Neill et al., 2001) which are most critical in coarse mode dominated conditions.

All operational stations in 2004 within our study domain that collected data on at least 30 h have been selected for the model evaluation. Table A2 and Fig. 1 describe and show the location and the main characteristics of the 35 selected AERONET localizations within our study region. Table A2 lists additional information including type of site, observation periods, percentage of cloud screened data and the availability of SDA products.

Quality-assured direct-sun data from all of the 440-870nm wavelength range is used to calculate the AOD at 550nm obtained by the Ångström's equation adjustment. The contribution of each aerosol fraction is analysed using the SDA retrieval products (AOD_{fine} and AOD_{coarse}).

3 Model evaluation

There is a number of metrics that can be used to examine performances of air quality models (US EPA, 1984, 1991; Cox and Tikvart, 1990; Weil et al., 1992; Chang and Hanna, 2004; Boylan and Russell, 2006; Dennis et al., 2010). Correlation coefficient

ACPD
11, 20575–20629, 2011

(r), root mean squared errors (RMSE), mean bias (MB) and normalize bias error (MNBE) are commonly used by the modelling community. For the evaluation of particulate matter concentrations, Boylan and Russell (2006) suggested the mean fractional bias (MFB) and the mean fractional error (MFE). They propose that a model performance goal is met when both the MFE and MFB are less than or equal to 50 % and ±30 %, respectively, and a model performance criterion is met when both MFE and MFB are less than or equal to 75 % and 60 %, respectively. The model-to-data statistics MB, MNBE, RMSE, MFE and MFB are selected for the present study, together with the measured and modelled mean and the correlation coefficient. The description of these statistics is presented in Table B1. Comparisons are made for annual and monthly basis as well as 4 seasonal periods: winter (DJF) corresponding to December, January and February, spring (MAM) corresponding to March, April and May, summer (JJA) corresponding to June, July, August and autumn (SON) corresponding to September, October and November. Measured aerosol surface concentrations and aerosol mass form EMEP/CREATE networks are available on a daily basis except for carbonaceous matter which are available on a annual basis. Moreover, since AERONET data are acquired at 15-min intervals on average, all AERONET measurements within ±30 min of the model outputs have been extracted and used for the model comparison at an hourly and daily basis.

Due to comparisons between simulations and observations present small differences among sites located in the same area, statistical indicators have been averaged over the regions indicated in Fig. 1 by colours and defined in Tables A1 and A2.

3.1 Ground level PM2.5 and PM10 concentrations

Before evaluating PM composition, it is important to ensure that reactive gases are well reproduced, since a major fraction of ambient PM arises from atmospheric gas-to-particle conversion (Meng et al., 1997). In Pay et al. (2010) the CALIOPE model output for gas and particulate phase concentrations are compared with ground-based measurements from the EMEP monitoring network for year 2004 over Europe. This

ACPD
11, 20575–20629, 2011

model evaluation showed that the modelling system is able to reproduce the general trends and daily variations of gas phase pollutants (SO_2, NO_2 and O_3).

In Table 1 and Fig. 2a, b, f, and g depict the annual and seasonal statistical results of the evaluation of PM and the evolution of the all-European average time series from model and observation. Although the model presents a clear systematic negative bias of PM2.5 (annual MB = $-6.30\,\mu g\,m^{-3}$), it is able to reproduce moderately well the daily evolution through the year ($r = 0.47$, Fig. 2a). Higher correlations are observed during wintertime and lower underestimations are detected in autumn (MB = $-5.0\,\mu g\,m^{-3}$).

PM10 is to a slightly larger extent underestimated (annual MB = $-10.30\,\mu g\,m^{-3}$) although the evolution over the year 2004 is well reproduced (Fig. 2b) with correlations ($r = 0.57$) higher than for PM2.5. PM10 includes the PM2.5 fraction, the primary anthropogenic coarse fraction as well as the contribution of coarse natural aerosols (i.e. SSA and desert dust). Higher PM10 correlations are observed in summertime and in the southern European stations affected by African dust outbreaks (see Fig. 3). The modelled desert dust contributions to PM2.5 and PM10 are on average 20 % and 25 %, respectively, increasing to 33 % and 35 % for Mediterranean stations.

The results obtained by the CALIOPE system for PM2.5 and PM10 are in the range of those shown in other European modelling studies (see Sect. 4 of the work of Pay et al., 2010). However, the MFE and MFB for PM2.5 and PM10 do not meet the performance criteria proposed by Boylan and Russell (2006). Many studies have recognized the difficulty of models to simulate the mass of particulate matter over Europe (Schaap et al., 2004; Matthias, 2008; Pay et al., 2010). The underestimation of total particulate mass is, among others, the result from the lack of fugitive dust emissions, resuspended matter, a possible underestimation of primary carbonaceous particles, the inaccuracy of SOA formation, the difficulty of representing primary PM emission from wood burning and other sources not considered in the emission inventory as pollutant sources over North Africa (Rodríguez et al., 2011) and a more general lack of process knowledge on aerosol removal and dispersion and transport processes.

ACPD
11, 20575–20629, 2011

3.2 PM chemical composition

Chemical composition measurements can help to identify model limitations in simulating the physical and chemical processes leading to the formation of SIA (namely, sulphates, nitrates and ammonium), SOA and SSA. For the sake of comparison with EMEP stations different size modes are lumped to obtain the total sulphate (Aitken, accumulation and coarse modes), nitrate (Aitken, accumulation and coarse modes), ammonium (Aitken and accumulation modes), chloride and sodium (accumulation and coarse modes) and carbonaceous matter concentration (i.e. organic and elemental carbon). Table 1, Figs. 2c–e, h–j and 3 show the annual and seasonal statistics as well as the all-European temporal evolution of the model and ground-level EMEP/CREATE measurement concentrations for SIA components calculated on a daily basis.

The overall annual variability of the modelled sulphate concentrations (Fig. 3) agrees as much as PM2.5 with measurements ($r = 0.49$), however with better results during summer ($r = 0.59$) when sulphate concentrations reach maximum levels due to enhanced photochemistry, low air mass renovation at regional scale and the increase of the summer mixing layer depth favouring the regional mixing of polluted air masses (Querol et al., 2009). On average, annual sulphate levels are underestimated by 18 %, thus smaller than PM2.5, with winter having the largest bias. Significant winter underestimations are located at stations in Eastern Europe (E.Eu region), where the mean bias per station ranges from $-0.5\,\mu g\,m^{-3}$ to $-2.5\,\mu g\,m^{-3}$ (Fig. 3). On the contrary, at stations in the region of France (S.Fr and C.Fr) and near the Northern Atlantic (N.Atl) the simulated sulphate exceeds the measurements by $0.3\,\mu g\,m^{-3}$ and $0.4\,\mu g\,m^{-3}$, respectively (Fig. 3). With respect to the temporal evolution the model presents the highest correlations in the Iberian Peninsula and Western Mediterranean Basin, ranging between 0.48 and 0.81 (see Fig. 3).

On average, modelled nitrate concentrations reproduce well the daily variability of the observations through the year ($r = 0.58$), presenting higher concentrations in winter and lower levels in summer due to its thermal instability (Querol et al., 2009). The

ACPD
11, 20575–20629, 2011

modelling system simulates lower aerosol nitrate concentrations than those measured (underestimations ~50 %), particularly in winter and spring (MB = −1.1 µg m^{-3}). On average, nitrate formation is limited by the availability of nitric acid over land, which may be related with the underestimation of the modelled NO_2 concentrations outlined and discussed in Pay et al. (2010). The largest underestimations are located over Eastern Iberian Peninsula-Western Mediterranean (E.IP-W.Med) and Central Mediterranean (C.Med) area with MB of −1.8 µg m^{-3} and Eastern Europe area (E.Eu region, except at Illmitz and Sniezka stations) with MB of −1.5 µg m^{-3} (Fig. 3). As in the case of sulphate, the model presents the best correlative skills over the Western Iberian Peninsula (W.IP) with relatively high correlations ranging from 0.40 to 0.65 by stations (Fig. 3), and annual MB and RMSE less than 1 µg m^{-3}.

In air masses with a continental signature, aerosol nitrate and sulphate are associated with ammonium (Schaap et al. 2004; Querol et al., 2009). Atmospheric ammonia is first neutralized by sulphuric acid to form ammonium sulphate. Remaining ammonia may then combine with nitric acid to form ammonium nitrate (Seinfeld and Pandis, 1998). Ammonium model comparison to measured data reveals that the annual variability is correctly reproduced (Fig. 2e), especially during autumn. However, the annual mean ammonium model concentration is low by 36 %, with the highest bias in winter (MB = −0.8 µg m^{-3}). However, the temporal variability is correctly captured during this season ($r = 0.70$). The overall variability of the modelled ammonium agrees fairly well with the measurements ($r = 0.62$, see Table 1 and Fig. 3).

For the sea salt component (i.e., sodium and chloride), the modelling system reproduces the daily variability with annual correlations for sodium and chloride of 0.67 and 0.46 respectively (Table 1 and Fig. 4). It should be noted that the results are strongly biased towards measurements obtained in northern Europe, since 9 out of 10 stations are located there (see Table A1). There are 4 coastal stations where the model simulates slightly higher chloride and sodium concentrations than those measured while at continental areas sea salt tends to be underestimated. Correlation for sodium is higher than for chloride since sodium is considered as inert in the atmosphere. One source

ACPD
11, 20575–20629, 2011

of uncertainty is related to the fact that AERO4 considers coarse mode aerosols as dry and inert. This approach does not allow important aerosol processes, such as the replacement of chloride by nitrate in mixed marine/urban air masses (Kelly et al., 2010) especially intense in summer when nitric acid is released by the thermal instability of ammonium nitrate (Querol et al., 2004). Moreover, degassing of Cl^- is not implemented in the model, and heterogeneous reactions are not taken into account. Transfer from PM10 to PM2.5 is also not considered in AERO4.

OC and EC are the major components of PM10 and PM2.5 in urban and kerbsites in central Europe (Putaud et al., 2004). Unfortunately, European measurements of carbonaceous aerosols are still sparse and unavailable. For OC and EC only two CREATE stations were available, Birkenes (NO01) and Melpitz (DE44), so the results of the carbonaceous aerosol are far from being representative and currently subject to re-evaluation by the EUSAAR project. The observed values are approximately a factor of 4 higher than the modelled values. This factor is higher than that obtained by Matthias (2008) at Birkenes in 2001 (factor of 3) partly because carbonaceous particles from biomass burning emissions were taken into account in the aforementioned study. There are other studies that demonstrate that SOA are underestimated by current models by a factor of 6 (Volkamer et al., 2006). The large uncertainties are associated with (1) the state-of-the-science concerning to SOA formation pathways (Eder and Yu, 2006; Edney et al., 2007; Wyat Appel et al., 2008) and (2) probable underestimation of primary carbonaceous emission (Cooke and Wilson, 1996; Bond et al., 2004; Schaap et al., 2004; Tsyro et al., 2007).

As a summary, the modelling system reproduces the daily variability of the main aerosol components in Europe. However their concentrations are in most cases strongly underestimated. The most important underestimations are observed for total carbonaceous material (i.e. OC and EC). The total amount of SIA is on average underestimated by 18–50 %. SSA is underestimated over inland and overestimated at coastal sites of northern Europe.

ACPD
11, 20575–20629, 2011

3.3 Aerosol optical depth

The evaluation of the AOD is particularly useful for validating the capabilities of the modelling system to reproduce European regional transport as well the long-range transport of desert dust from North Africa at high altitudes.

The modelling system is quantitatively compared against direct-sun AOD measurements (AOD) and the AOD mode products from the SDA retrieval (AOD_{fine} and AOD_{coarse}). AOD_{fine} corresponds to sub-micron aerosols and AOD_{coarse} corresponds to super-micron aerosols. Modelled AOD_{fine} includes ammonium, sulphate, nitrate, SSA, OC and EC as well unspeciated mass fine portion from CMAQ as well sub-micron desert dust from BSC-DREAM8b, meanwhile, modelled AOD_{coarse} is the sum of the super-micron fraction of desert dust from BSC-DREAM8b and SSA and unspeciated mass coarse portion from CMAQ. Table 2 and Fig. 5 show the annual and seasonal statistics as well as the temporal evolution of the model and ground-based AERONET measurements for AOD, AOD_{fine} and AOD_{coarse} calculated on an hourly and daily basis.

The model reproduces the AOD hourly and daily variability with an annual correlation of 0.51 and 0.56 respectively on average (Table 2, Figs. 5a and 6) and underestimates the hourly and daily AOD by 41 and 38 % respectively (Table 2, Figs. 5a and 6). In contrast to the PM evaluation, the annual MFB and MFE (see Table 2) meet the recommendations proposed by Boylan and Russell (2006) indicating satisfactory performances for the modelled AOD.

If we take a closer look to the desert dust component and its role on the model data agreement, its influence is remarkable. When considering only CMAQ outputs the annual simulated AOD underestimation rises up to 61 % for houly values and 58 % for daily values and the annual correlation decreases to 0.39 for the hourly values and to 0.40 for daily values. Due to the proximity to the African continent, the differences between CMAQ-alone and CMAQ + BSC-DREAM8b are larger in the Iberian Peninsula and Mediterranean sites. Correlations remarkably improve from 0.16 to 0.59, 0.39 to 0.58, 0.31 to 0.49 and 0.05 to 0.50, for the Western Iberian Peninsula, Eastern Iberian

ACPD
11, 20575–20629, 2011

Peninsula-Western Mediterranean, Central Mediterranean and Eastern Mediterranean, respectively for hourly values. Averaging for the entire study region, desert dust contributions represent ~35 % of the AOD and over the Iberian Peninsula and Mediterranean ~51 % on average. These results are consistent with the aerosol characterization presented in Basart et al. (2009).

Because the evaluation of the aerosol model performance is hampered by the lack of routine data above the surface, satellite observations offer new opportunities for model evaluation. In Fig. 7, the seasonal averages for 2004 of the collection C005 AOD data (cloud free) at 550 nm from MODIS/Aqua sensor (Levy et al., 2003; Remer et al., 2005) are qualitatively compared with the modelled aerosol fields. Additionally, superimposed to MODIS values, the AERONET seasonal mean values are included showing moderate differences between both observational datasets. Among other causes, this is partly because the satellite product being obtained from 2 images per day as a difference of AERONET measurements.

The model reproduces moderately well the main seasonal AOD patterns observed in MODIS AOD product despite of the important underestimations at hot spots located in Northern Italy, Eastern and North-western Europe as shown in the comparison with AERONET data. The dust transport from North Africa is well captured with maximum AOD values in the Eastern Mediterranean region in spring shifting to Central and Western Mediterranean regions in summer.

The aerosol fields obtained with CALIOPE are similar to those shown in other European modelling studies (e.g., POLYPHEMUS; Tombette et al., 2008; CHIMERE, Péré et al., 2010). In another study with CMAQ (Matthias, 2008), the modelled AOD was 20–70 % lower than AERONET observations. In contrast to our results, the best scores in this study were achieved in northern sites where desert dust contributions are smaller, which again highlights the importance of desert dust in southern latitudes. The evaluation of the POLYPHEMUS system (Tombette et al., 2008), which also did not consider desert dust, against 19 AERONET stations underestimated the hourly AOD average from 0.02 to 0.07 and correlations ranged from 0.40 to 0.87 obtaining the best results

ACPD
11, 20575–20629, 2011

in the northern European sites. In the evaluation of the CHIMERE model against 13 AERONET stations presented in Péré et al. (2010), correlations lied within the range of 0.50–0.74 .The values obtained in the present work lie within the range of these studies with correlations of 0.40–0.72 depending on the region.

We take a closer look now at the fine and coarse components of the AOD. The annual and seasonal statistical results obtained for AOD_{fine} and AOD_{coarse} are presented in Table 2 and Fig. 6 and the temporal series are shown in Fig. 5b and c, respectively. The modelled desert dust contributions to AOD_{fine} and AOD_{coarse} are on average 22 % and 88 %, respectively. The largest discrepancies between model and data are associated to AOD_{fine} (MB = −0.13 and RMSE = 0.19, Table 2), but the hourly variability is reasonably well captured ($r = 0.52$, see Figs. 5b and 6). The best scores are found in SMHI site in the Nordic region ($r = 0.70$, RMSE = 0.04 and MB = −0.03) where no desert dust is present in the fine mode AOD and where the frequent background situation is associated with low values. The largest error in AOD_{fine} is found for Northern Italy (RMSE = 0.29 and MB = −0.20). The correlation remains moderately high though (∼0.52) indicating that the modelling system is able to reproduce reasonably well the background AOD and the timing of the sudden increases. Northern Italy includes one of the most polluted regions in Europe, the Po Valley (Mélin and Zibordi, 2005) and the model indicates almost no contribution from dust (desert dust contributions to AOD less than 4 %) in agreement with the results of the aerosol characterization from Gobbi et al. (2007). In this area, the air stagnation in a mountain-surrounded valley favours the photochemical reactions that produce SIA and the fine mode growth (Gobbi et al., 2007) together with frequent humid conditions in winter which challenges models.

The overall annual variability of the modelled AOD_{coarse} agrees fairly well with measurements ($r = 0.63$, see Fig. 5c). The best scores are found in the Mediterranean Basin ($0.6 < r < 0.8$, RMSE < 0.09 and MB ∼ −0.04, on average in hourly mean values for the entire Basin) particularly in summertime coinciding with the maximum AOD_{coarse} values and maximum activity in the desert dust sources (Middelton and Goudie, 2001). The largest discrepancies are found in Nordic countries ($r = 0.06$, RMSE = 0.03 and

ACPD
11, 20575–20629, 2011

MB = −0.02) and Eastern Europe (r = 0.18, RMSE = 0.10 and MB = −0.06).

The ESCOMPTE experiment (Mallet et al., 2003), which investigated the microphysical and optical properties of the aerosol around Marseille in the summer 2001, showed that 90 % of the light extinction is due to anthropogenic aerosol and only 10 % is due to natural aerosol (SSA and desert dust). 44 % of the anthropogenic extinction was due to ammonium sulphates, followed by 20 % from EC and 21 % by OM. Nitrate aerosol had a weak contribution (∼5 %). In the present study, at the Western Mediterranean sites (i.e. AVI, CAR, TUL and VIL) during the summer months of the year 2004, 28 % of the light extinction is due to natural aerosol (SSA and desert dust) and 72 % is due to anthropogenic aerosol. In our model, 54 % of the anthropogenic extinction is due to ammonium sulphates, followed by nitrate (∼13 %) and EC and OC with ∼6 % and ∼9 %, in that order. These results reveal important underestimates of total carbonaceous material (i.e. EC + OC) species. The important underestimations of EC and OC can be partly explained by the influence of local emissions and natural sources. The uncertainties associated to the emission inventory for black carbon may be an important cause for the discrepancy (Schaap et al., 2004; Baldasano et al., 2008b).

4 Aerosol distribution over Europe

4.1 Model bias correction

Several studies have demonstrated the benefit of adjusting site-specific air quality model predictions using observational data to reduce systematic model error (e.g. Hogrefe et al., 2006; Djalalova et al., 2010). Bias-adjustment strategies range from the relatively simple mean bias and multiplicative ratio adjustments used by McKeen et al. (2005) to the more complex Kalman Filter techniques (Manders et al., 2009; Kang et al., 2010; Sicardi et al., 2011). In the present section, we intend to provide an estimation of the spatial and seasonal distribution of the different aerosol fractions over Europe with our model results including an a posteriori correction. The evaluation

ACPD
11, 20575–20629, 2011

(see Sect. 3) consistently reveals a similar degree of fine fraction underestimation on both surface levels and column-integrated values (AOD). In this regard, the correction applied use the results of the evaluation against measured chemical aerosol surface concentrations on total mass fraction on a daily basis described in the Sect. 2.3.1.

We calculate spatially homogeneous, for all Europe, multiplicative correction factors per aerosol species and apply it to the mass concentrations in the model. The main limitation of this method is the application of a spatially homogeneous correction factor for a large region such as Europe. However, as described below the modelled bulk parameters: PM levels and AOD, significantly improve after correcting the bias of each aerosol species individually.

For carboneous compounds (i.e. EC and OC), a spatially homogeneous mean annual multiplicative correction factor of 4 is estimated (see Sect. 3.2). For the SIA (i.e. sulphates, nitrates and ammonium) components the correction factor is calculated from the modelled and observed mean daily values. We employ a weighted sum of the squared difference between the modelled and observed values. We minimize this sum to identify the magnitude of the aerosol concentration that is in optimal agreement with the observations. Table 3 shows the spatially homogeneous multiplicative correction factors obtained for each chemical species. The bias corrected simulation is then evaluated against the bulk PM and AOD observations from EMEP and AERONET respectively (Table 4).

The corrected PM2.5 and PM10 results present a much better agreement with the observations if correction factors are applied (Fig. 2 and Table 4). The annual underestimations are reduced from 53 % to 18 % for PM2.5 and from 58 % to 35 % for PM10. Correlations increase from 0.47 to 0.59 for PM2.5 and from 0.57 to 0.61 for PM10. In fact, the MFE and MFB for the corrected PM2.5 fall within the performance goal meanwhile the corrected PM10 fall within the performance criterion proposed by Boylan and Russell (2006). Correlation, RMSE, MFB and MFE of PM2.5 and PM10 with correction factors are significantly better than those obtained in Pay et al. (2010) by applying a factor of 2 to total PM2.5 and PM10.

ACPD
11, 20575–20629, 2011

The annual underestimations are reduced from 57 % to 32 % for hourly AOD_{fine} and from 41 % to 13 % for hourly AOD while correlations increase from 0.52 to 0.56 for hourly AOD_{fine} and from 0.51 to 0.56 for hourly AOD (Table 2 and Figs. 5 and 6). Similar results are obtained for daily AOD and AOD_{fine} (see Table 4). Finally, Fig. 7 highlights the closer agreement of the model corrected seasonal AOD distribution with the MODIS/Aqua satellite product in comparison with the uncorrected model estimates. The corrected simulation provides more realistic information for the analysis of the aerosol spatial and temporal patterns over Europe.

4.2 Spatial and seasonal distribution of aerosol fractions

Fig. 8 shows the modelled annual mean of PM2.5, PM10, AOD and AOD_{fine}. The highest annual mean aerosol concentrations ($AOD > 0.3$ and $PM10 > 30\,\mu g\,m^{-3}$) are found over the Po Valley and the Benelux region (Belgium, The Netherlands, Luxembourg) where values are dominated by fine anthropogenic aerosols. To a lesser extent, a second maximum is found over South-eastern Europe, namely in Greece, Macedonia, Bulgaria and Rumania, and over the Moldavia, Ukraine, and Poland ($AOD \sim 0.2$) and southern Europe ($AOD > 0.2$ and $PM10 > 20\,\mu g\,m^{-3}$). Aerosol concentrations decrease towards the North and North-western Europe reaching the lowest values in the northern region ($AOD < 0.15$) in agreement with the modelling study of Schaap et al. (2004). Low values are also found over the major European mountain chains (e.g. the Alps, Massif Central, the Pyrenees and the Carpathians) with $AOD < 0.1$ and $PM10 < 10\,\mu g\,m^{-3}$.

We distinguish some common features in the column-integrated and surface distributions such as the high values over the North of Italy and the Netherlands. There are also significant contrasts as for instance the maritime areas in the North Atlantic region and Eastern Europe. Differences over the North Atlantic region are associated to the relatively low SSA extinction (Dubovik et al., 2002) in comparison to its impact on PM10 values. Over the continent, differences between PM surface concentrations and AOD are partly due to the dilution conditions related to the PBL height due to changes in the

ACPD
11, 20575–20629, 2011

vertical mixing and to the moisture content affecting the optical properties of aerosols (Gupta and Christopher, 2009). On the other hand, aerosols in the free troposphere are transported from other regions, significantly contributing to the total AOD (e.g. Amiridis et al., 2005).

Figures 9 and 10 present the mean seasonal PM10 and AOD together with the fractions of anthropogenic (nitrate, sulphate, ammonium and OC + EC) and natural aerosols (SSA and desert dust).

Despite SO_x emissions are rather constant throughout the year, a clear seasonal trend is observed in the modelled sulphate PM and AOD during the warm season due to high temperature and low relative humidity that favour the oxidation of SO_2 and the formation of sulphate under the presence of hydroxyl radical (e.g. Querol et al., 2009). In summer, sulphate AOD reaches average values above 0.12 in Eastern Europe, with a maximum of 0.28 over Rumania. High surface concentrations of sulphate are calculated in summer over the Aegean Sea (~5 $\mu g\,m^{-3}$) due to the shipping traffic emissions and over the Balkans regions (above 5 $\mu g\,m^{-3}$) due to emissions from power plants.

Nitrate levels present a strong seasonal variability with the highest values during the cold months (Figs. 9 and 10). In winter nitrate contributions to PM levels and AOD up to 40 % are observed over the entire European continent. In summer the highest contributions are localised in the Central Europe. Ammonium concentration shows slight variations throughout the year (Figs. 9 and 10). The highest contributions to PM and AOD (~15 % and ~20 %, respectively) are observed in winter and the lowest contributions (<10 %) in summer. Maximum surface concentrations of nitrate (~4.6 $\mu g\,m^{-3}$) and ammonium (~3 $\mu g\,m^{-3}$) are simulated over most European countries in winter, with the highest levels over the Po Valley (>8 $\mu g\,m^{-3}$ and >5 $\mu g\,m^{-3}$ for nitrates and ammonium, respectively). Their maximum contribution to AOD is found in the Po Valley (~0.10) and to a lesser extent in the Benelux area (~0.08).

OC + EC estimations should be taken with precaution due to the bad skills of models and the lack of observations over Europe. OC + EC are concentrated at hot spot locations where they are found in the fine fraction with maximum PM2.5 values of ~6 $\mu g\,m^{-3}$

ACPD
11, 20575–20629, 2011

and AOD_{fine} values up to 0.01. Maximum OC + EC contributions are observed in summer (Figs. 9 and 10). Also, SSA contributes weakly to the AOD with an average mean annual value of less than 0.01. At surface levels, the mean contribution of SSA to PM10 in the Mediterranean Sea reaches up to 40 % (~10 $\mu g\,m^{-3}$) and up to 80 % (15 $\mu g\,m^{-3}$) in the North Atlantic.

Sulphates and nitrates contribute up to 80 % of the PM10 and AOD in latitudes beyond 41° N (Figs. 9 and 10). Maxima SIA and carbonaceous matter are mainly concentrated at hot spot localizations in Europe where they are found in the fine fraction.

In contrast to anthropogenic sources, which are mainly located in the European continent, mineral dust sources affecting Europe's PM levels are mostly found in North African deserts. One distinct feature of the CALIOPE modelling system with respect to other European systems is the inclusion of the influence of African dust on a non-climatologically basis by means of the offline coupling with the BSC-DREAM8b model. Desert dust exhibits a strong seasonal variability throughout the year. Maximum desert dust transport to Europe occurs from spring to early autumn according to the model results (Figs. 9 and 10), while minimum desert dust contributions are found in winter over the entire region. In spring, an increase of dust outbreaks and high desert dust contributions (>40 %) are observed in the Central and Eastern Mediterranean regions. In summer, the maximum desert dust contribution is shifted towards the Western Mediterranean and the Southern Iberian Peninsula. In the South-eastern Iberian Peninsula, desert dust contributes about 60–70 % of the PM10 and AOD levels which reach 40 $\mu g\,m^{-3}$ and 0.2, respectively (Figs. 9 and 10).

The simulated seasonal patterns are in agreement with observational studies using ground-based (e.g. Papayannis et al., 2008; Basart et al., 2009) and satellites observations (e.g. Barnaba and Gobbi, 2004; Antoine and Nobileau, 2006). Long-range transport of Saharan dust across the United Kingdom appears to be much less frequent than for Southern and Central Europe (Ryall et al., 2002) as a consequence of typical atmospheric circulation patterns. Dust particles penetrate to Northern Europe reaching the United Kingdom and the North Sea in winter (contributions to PM10

ACPD
11, 20575–20629, 2011

~15 % in northern United Kingdom in winter see Fig. 9).

African dust outbreaks have been long recognized to cause exceedances of the European air quality thresholds (Rodríguez et al., 2001; Barnaba and Gobbi, 2004; Querol et al., 2004; Papanastasiou et al., 2010). In Fig. 11 we provide a spatial estimate of the number of days in which the daily European air quality threshold (50 $\mu g\,m^{-3}$) is exceeded due to natural dust events. Fig. 11a provides an estimate based only on desert dust levels. Large regions from Iberian Peninsula to Greece (in the North Mediterranean arc, <45° N) exceed the threshold while the number of daily exceedances increases southwards reaching up to about 75 days per year in the southernmost areas. When we include the other aerosol components (Fig. 11b), a significant number of exceedances appear in well-known European hot spots. In particular, the threshold is exceeded more than 75 days in the Po Valley, Eastern Europe and in the Benelux regions. Additionally in those regions most affected by the presence of desert dust (in the North Mediterranean arc, <45° N), the number of exceedances notably increases with respect to the desert dust only case achieving up to 100 days in mountainous areas in the southeastern Iberian Peninsula. We note that Fig. 11b may only represent a lower end estimate of the total number of exceedances given that the PM10 mass is significantly underestimated in the modelling system (about 6 $\mu g\,m^{-3}$ on average).

5 Summary and conclusions

We have presented a detailed aerosol evaluation and characterization over Europe for year 2004 using the CALIOPE modelling system. We performed a detailed model evaluation of PM levels, AOD and chemical composition to quantify the model skills and identify the causes of discrepancy.

The aerosol evaluation against EMEP/CREATE and AERONET networks shows that the modelling system can reproduce reasonably well the daily variability of the main aerosol components in Europe. However aerosol levels are in most cases underestimated. On the one hand, the larger underestimation in PM10 compared with PM2.5

ACPD
11, 20575–20629, 2011

suggests missing aerosol sources in the modelling system, which affect mainly these larger fractions. On the other hand, the evaluation of the chemical composition highlights important underestimations of the modelled fine fractions particularly for carbonaceous matter (EC and OC; underestimations ~200 %) and SIA (i.e. nitrates, sulphates and ammonium; the total amount of SIA is on average underestimated by 18–50 %).

We calculated spatially homogenous multiplicative correction factors for carboneous matter (EC and OC) and SIA components that minimize the differences between the modelled and observed values. The results of the corrected simulation highlight the fact that besides increasing the total mass budget (the annual underestimations are reduced by ~35 % and 23 % for PM2.5 and PM10, respectively), the correction by species improves the simulation of the variability of the bulk parameters with respect to the observed values (the annual correlation increases from 0.47 to 0.59 for PM2.5, and 0.57 to 0.61 and PM10, respectively). Also the corrected model AOD is significantly improved when compared to MODIS satellite AOD fields.

Aerosols over Europe are dominated by (1) local anthropogenic emissions, (2) the proximity to the African desert and (3) atmospheric dynamics at synoptic scale. The mean annual particulate matter concentration decreases towards the North and North-Western Europe reaching the lowest values in the northernmost regions. The highest aerosol concentrations are found over the industrialized and populated areas of the Po Valley and the Benelux regions. A second maximum is detected over Eastern and Southern Europe. High values in southern Europe are linked to the transport of large particles from Sahara desert. Maximum values are found in spring in the Eastern Mediterranean and in summer over the Iberian Peninsula and the Central-western Mediterranean. SIA are concentrated in the fine fractions and they are the main contributors to the aerosol mass budget in the European continent reaching up to 80 % for latitudes beyond 40° N.

We have shown the importance of the desert dust transported from North Africa in the aerosol budget in southern European countries. We estimate that the presence of mineral dust from African deserts cause exceedances of the daily PM10 European air

ACPD
11, 20575–20629, 2011

quality threshold (50 µg m^{-3}) in latitudes south of 45° N reaching up to more than 75 days per year in the southernmost regions.

Despite the rather satisfactory performance of the modelling system, several aspects are now under further implementation in the framework of the CALIOPE project. Wind-blown dust should be taken into account especially in dry and arid regions as well resuspension from paved roads in urban areas (see Pay et al., 2011). Biomass burning and natural NO_x are currently not treated in the CALIOPE modelling system and could contribute to the NO_2 underestimation. The uncertainties associated to the emission inventory for black carbon may be an important cause for the discrepancy between observed and modelled values; however, the uncertainties in the state-of-the-science of SOA formation and in the equilibrium sulphate/nitrate/ammonium should be further investigated. We also expect further improvements in the secondary organic aerosol formation and the dynamic interactions of fine and coarse aerosol with the new version of CMAQ (CMAQv4.7) that features a new aerosol module, AERO5, containing substantial scientific improvements over the AERO4 released in version 4.5.

Appendix A

List of observational stations

Tables A1 and A2 describe the location and the main characteristics of the 54 selected EMEP and 35 selected AERONET localizations within our study region. Table A1 includes the main characteristics and location of the EMEP/CREATE stations and Table A2 lists additional information including type of site, observation periods, percentage of cloud screened data and the availability of SDA products of the AERONET stations.

ACPD
11, 20575–20629, 2011

Appendix B

Definition of the statistics

The description of the statistics used in the present analysis for the model evaluation are shown in Table B1.

Acknowledgements. The authors wish to thank EMEP and AERONET for the provision of measurements stations and CIEMAT, CSIC-IJA, CEAM centers for their collaboration in the CALIOPE project. We also acknowledge the MODIS mission scientists and associated NASA personnel for the production of the data used in this research effort. Also, special thanks to N. Clave as well M. Piot, L. González and S. Gassó for their work related to the CALIOPE system and S. Szopa and A. Cozic for the provision of LMDz-INCA2 chemical data. This work is partially funded by the CALIOPE project of the Spanish Ministry of the Environment (441/2006/3-12.1, A357/2007/2-12.1, 157/PC08/3-12.0) and the project CICYT CGL2010-19652 of the Spanish Ministry of Education and Science. P. Jiménez-Guerrero acknowledges the Ramón y Cajal Programme of the Spanish Ministry of Science and Technology. All simulations were performed on the MareNostrum supercomputer hosted by the Barcelona Supercomputing Center-Centro Nacional de Supercomputación.

References

Amiridis, V., Balis, D. S., Kazadzis, S., Bais, A., Giannakaki, E., Papayannis, A., and Zerefos, C.: Four-year aerosol observations with a Raman lidar at Thessaloniki, Greece, in the framework of European Aerosol Research Lidar Network (EARLINET), Geophys. Res, 110, 1–12, 2005.

Amiridis, V., Kafatos, M., Perez, C., Kazadzis, S., Gerasopoulos, E., Mamouri, R. E., Papayannis, A., Kokkalis, P., Giannakaki, E., and Basart, S.: The potential of the synergistic use of passive and active remote sensing measurements for the validation of a regional dust model, Ann. Geophys, 27, 3155–3164, 2009.

Antoine, D. and Nobileau, D.: Recent increase of Saharan dust transport over the Mediterranean Sea, as revealed from ocean color satellite (SeaWiFS) observations, Geophys. Res., 111, D12214, doi:10.1029/2005JD006795, 2006.

ACPD

11, 20575–20629, 2011

Baldasano, J. M., Jiménez-Guerrero, P., Jorba, O., Pérez, C., López, E., Güereca, P., Martín, F., Vivanco, M. G., Palomino, I., Querol, X., Pandolfi, M., Sanz, M. J., and Diéguez, J. J: Caliope: an operational air quality forecasting system for the Iberian Peninsula, Balearic islands and Canary islands e first annual evaluation and ongoing developments, Adv. Sci. Res., 2, 89–98, 2008a.

Baldasano, J. M., Güereca, L. P., López, E., Gassó, S. and Jimenez-Guerrero, P.: Development of a high-resolution (1 km × 1 km, 1 h) emission model for Spain: The High-Elective Resolution Modelling Emission System (HERMES), Atmos. Environ., 42, 7215–7233, 2008b.

Baldasano, J. M., Piot, M., Jorba, O., Goncalves, M., Pay, M. T., Basart, S., Jiménez, P., and Gassó, S. CALIOPE: an Operational Air Quality Forecasting System for Europe and Spain. Mesoscale Modelling For Air Pollution Applications: Achievements And Challenges (COST 728 Final Workshop), Organisers: COST 728, WMO/GURME and MEGAPOLI, Geneva, 25–26, February 2010.

Barnaba, F. and Gobbi, G. P.: Aerosol seasonal variability over the Mediterranean region and relative impact of maritime, continental and Saharan dust particles over the basin from MODIS data in the year 2001, Atmos. Chem. Phys., 4, 2367–2391, doi:10.5194/acp-4-2367-2004, 2004.

Basart, S., Pérez, C., Cuevas, E., Baldasano, J. M., and Gobbi, G. P.: Aerosol characterization in Northern Africa, Northeastern Atlantic, Mediterranean Basin and Middle East from direct-sun AERONET observations, Atmos. Chem. Phys., 9, 8265–8282, doi:10.5194/acp-9-8265-2009, 2009.

Binkowski, F. S. and Roselle, S. J.: Models-3 Community Multiscale Air Quality (CMAQ) model aerosol component. 1. Model description, J. Geophys. Res., 108(D6), 4183, doi:10.1029/2001JD001 409, 2003.

Binkowski, F. S.: Aerosols in MODELS-3 CMAQ, in Science Algorithms of the EPA Models-3 Community Multiscale Air Quality (CMAQ) Modeling System, edited by: Byun, D. W. and Ching, J. K. S., 10-0–10-23, EPA, 1999.

Bond, T. C., Streets, D. G. Yarber, K. F., Nelson, S. M., Woo, J. H., and Klimont, Z.: A technology-based global inventory of black and organic carbon emissions from combustion, J. Geophys. Res. Atmos., 109, D14203, doi:10.1029/2003JD003697, 2004.

Boylan, J. W. and Russell, A. G.: PM and light extinction model performance metrics, goals, and criteria for three-dimensional air quality models, Atmos. Environ., 40, 4946–4959, 2006.

Byun, D. W. and Ching, J. K. S.: Science Algorithms of the EPA Models-3 Community Multiscale

ACPD
11, 20575–20629, 2011

Air Quality (CMAQ) Modeling System, Atmospheric modeling division, National Exposure Research Laboratory, US Environmental Protection Agency, Research Triangle Park, NC, 27711, 1999.
Byun, D. W. and Schere, K. L.: Review of the Governing Equations, Computational Algorithms, and Other Components of the Models-3 Community Multiscale Air Quality (CMAQ) Modeling System, Appl. Mech. Rev., 51–77, 2006.
Chang, J. C. and Hanna, S. R.: Air quality model performance evaluation, Meteor. Atmos. Phys., 87, 167–196, 2004.
Cooke, W. F. and Wilson, J. J. N.: A global black carbon aerosol model, J. Geophys. Res. Atmos., 101, 19395–19409, 1996.
Cox, W. M. and Tikvart, J. A.: A statistical procedure for determining the best performing air quality simulation model, Atmos. Environ. Part A. General Topics, 24, 2387–2395, 1990.
Dennis, R., Fox, T., Fuentes, M., Gilliland, A., Hanna, S., Hogrefe, C., Irwin, J., Rao, S. T., Scheffe, R., and Schere, K.: A framework for evaluating regional-scale numerical photochemical modeling systems, Environ. Fluid Mechanics, 1–19, 2010.
Djalalova, I., Wilczak, J., McKeen, S., Grell, G., Peckham, S., Pagowski, M., Delle Monache, L., McQueen, J., Tang, Y., Lee, P., McHenry, J., Gong, W., Bouchet, V., and Mathru, R.: Ensemble and bias-correction techniques for air quality model forecasts of surface O_3 and PM2.5 during the TEXAQS-II experiment of 2006, Atmos. Environ., 44, 455–467, 2010.
Dubovik, O. and King, M. D.: A flexible inversion algorithm for retrieval of aerosol optical properties from sun and sky radiance measurements, J. Geophys. Res., 105(D16), 20676, doi:10.1029/2000JD900282, 2000.
Dubovik, O., Holben, B. N., Eck, T. F., Smirnov, A., Kaufman, Y. J., King, M. D., Tanré, D., and Slutsker, I.: Variability of Absorption and Optical Properties of Key Aerosol Types Observed in Worldwide Locations, Atmos. Sci., 59, 590–608, 2002.
Eder, B. and Yu, S.: A performance evaluation of the 2004 release of models-3 CMAQ, Atmos. Environ. 40, 4811–4824. doi:10.1016/j.atmosenv.2005.08.045, 2006.
Edney, E. O., Kleindienst, T. E., Lewandowski, M., and Offenberg, J. H.: Updated SOA chemical mechanism for the community multi-scale air quality model, EPA 600/X-07/025, US Environmental Protection Agency, Research Triangle park, North Carolina, 2007.
EMEP: National Emissions Reported to the Convention on Long-range Transboundary Air Pollution (LRTAP Convention). Air Emission Annual Data Reporting (EMEP/MSC-W). Technical Report, European Environmental Agency, The Norwegian Meteorological Institute, Oslo,

ACPD
11, 20575–20629, 2011

Norway, 2007.
European Commission: Directive 2008/50/EC of the European Parliament and of the Council of 21 May 2008 on Ambient Air Quality and Cleaner Air for Europe, Technical Report 2008/50/EC, L152. Off. J. Eur. Comm., 2008.
Gery, M. W., Whitten, G. Z., Killus, J. P., and Dodge, M. C.: A photochemical kinetics mechanism for urban and regional scale computer modeling, J. Geophys. Res., 94(D10), 12925–12956, 1989.
Gobbi, G. P., Kaufman, Y. J., Koren, I., and Eck, T. F.: Classification of aerosol properties derived from AERONET direct sun data, Atmos. Chem. Phys., 7, 453–458, doi:10.5194/acp-7-453-2007, 2007.
Gong, S. L.: A parameterization of sea-salt aerosol source function for sub- and super-micron particles, J. Geophys. Res., 17, 1097, doi:10.1029/2003GB002 079, 2003.
Gupta, P. and Christopher, S. A.: Particulate matter air quality assessment using integrated surface, satellite, and meteorological products: Multiple regression approach, J. Geophys. Res., 114, D14205, doi:10.1029/2008JD011496, 2009.
Hogrefe, C., Hao, W., Civerolo, K., Ku, J. Y., and Sistla, G: Exploring approaches to integrate observations and CMAQ simulations for improved air quality forecasts, Presented at the 5th nnual CMAQ User's Conference, Chapel Hill, NC. Available on the Internet at http://www.cmascenter.org/conference/2006/abstracts/hogrefe_session3.pdf, 2006.
Haustein, K., Pérez, C., Baldasano, J. M., Müller, D., Tesche, M., Schladitz, A., Esselborn, M., Weinzierl, B., Kandler, K., and Hoyningen-Huene, W. v.: Regional dust model performance during SAMUM 2006, Geophys. Res. Lett., 36, L03812, doi:10.1029/2008GL036463, 2009.
Holben, B. N., Eck, T. F., Slutsker, I., Tanré, D., Buis, J. P., Setzer, A., Vermote, E., Reagan, J., Kaufman, Y., Nakajima, T., Lavenu, F., Jankowiak, I., and Smirnov, A.: AERONET: A Federated Instrument Network and Data Archive for Aerosol Characterization, Rem. Sens. Environ., 66, 1–16, 1998.
IPCC, Intergovernmental Panel on Climate Change: Climate change 2007: Synthesis Report, http://www.ipcc.ch/pdf/assessment-report/ar4/syr/ar4syr.pdf, 2007.
Jiménez, P., Baldasano, J. M., and Dabdub, D.: Comparison of photochemical mechanisms for air quality modelling, Atmos. Environ., 4179–4194, doi:10.1016/S1352–2310(03)00, 567–3, 2003.
Jiménez-Guerrero, P., Jorba, O., Baldasano, J. M., and Gassó, S.: The use of a modelling system as a tool for air quality management: Annual high-resolution simulations and evaluation,

ACPD
11, 20575–20629, 2011

Science of the Total Environment, 390(2–3), 323–340, 2008.
Kang, D., Mathur, R., and Rao, S. T.: Assessment of bias-adjusted PM2. 5 air quality forecasts over the continental United States during 2007, Geosci. Model Dev., 3, 309–320, 2010.
Kelly, J. T., Bhave, P. V., Nolte, C. G., Shankar, U., and Foley, K. M. Simulating emission and chemical evolution of coarse sea-salt particles in the Community Multiscale Air Quality (CMAQ) model, Geosci. Model Dev. 3, 257–273, 2010.
Larssen, S., Sluyter, R., and Helmis, C.: Criteria for EUROAIRNET, the EEA Air Quality Monitoring and Information Network. Technical Report No. 12. European Environment Agency, http://reports.eea.eu.int/TEC12/en, 1999.
Levy, R. C., Remer, L. A., Tanré, D., Kaufman, Y. J., Ichoku, C., Holben, B. N., Livingston, J. M., Russell, P. B., and Maring, H.: Evaluation of the Moderate-Resolution Imaging Spectroradiometer (MODIS) retrievals of dust aerosol over the ocean during PRIDE, J. Geophys. Res., 108(D19), 8594, doi:10.1029/2002JD002460, 2003.
Mallet, M., Roger, J. C., Despiau, S., Dubovik, O., and Putaud, J. P.: Microphysical and optical properties of aerosol particles in urban zone during ESCOMPTE, Atmos. Res., 69, 73–97, 2003.
Malm, W. C., Sisler, J. F., Huffman, D., Eldred, R. A., and Cahill, T. A.: Spatial and seasonal trends in particle concentration and optical extinction in the United States, J. Geophys. Res., 99, 1347–1370, 1994.
Manders, A. M. M., Schaap, M., and Hoogerbrugge, R.: Testing the capability of the chemistry transport model LOTOS-EUROS to forecast PM10 levels in the Netherlands, Atmos. Environ., 43(26), 4050–4059, 2009.
Matthias, V.: The aerosol distribution in Europe derived with the Community Multiscale Air Quality (CMAQ) model: comparison to near surface in situ and sunphotometer measurements, Atmos. Chem. Phys., 8, 5077–5097, doi:10.5194/acp-8-5077-2008, 2008.
McKeen, S., Wilczak, J., Grell, G., Djalalova, I., Peckham, S., Hsie, E. Y., Gong, W., Bouchet, V., Menard, S., Moffet, R., McHenry, J., McQueen, J., Tang, Y., Carmichael, G. R., Pagowski, M., Chan, A., Dye, T., Frost, G., Lee, P., and Mathur, R.: Assessment of an ensemble of seven real-time ozone forecasts over eastern North America during the summer of 2004, J. Geophys. Res., 110, D21307, doi: 10.1029/2005JD005858, 2005.
Medina, S., Le Tertre, A., and Saklad, M.: The APHEIS Project: air pollution and health – a European information system, Air Quality, Atmosphere & Health, 2, 185–198, 2009.
Mélin F. and Zibordi, G.: Aerosol variability in the Po Valley analyzed from automated optical

ACPD
11, 20575–20629, 2011

measurements, Geophys. Res. Lett., 32, L03810, doi:10.1029/2004GL021787, 2005.
Meng, Z., Dabdub, D., and Seinfeld, J. H.: Chemical coupling between atmospheric ozone and particulate matter, Science, 277,5322, 116–119, doi:10.1126/science.277.5322.116, 1997.
Menut, L. and Bessagnet, B.: Atmospheric composition forecasting in Europe, Ann. Geophys., 28, 61–74, 2010, http://www.ann-geophys.net/28/61/2010/.
Middleton, N. J. and Goudie, A. S.: Saharan dust: sources and trajectories, Trans. Inst. Br. Geogr., 26, 165, doi:10.1111/1475-5661.00013, 2001.
Nenes, A., Pilinis, C., and Pandis, S. N.: ISORROPIA: A New Thermodynamic Equilibrium Model for Multiphase Multicomponent Inorganic Aerosols, Aquatic Geochemistry, 4(1), 123–152, doi:10.1023/A:1009604003981, 1998.
Nickovic, S., Kallos, G., Papadopoulos, A., and Kakaliagou, O.: A model for prediction of desert dust cycle in the atmosphere, J. Geophys. Res., 106(D16), 18113–18129, doi:10.1029/2000JD900794, 2001.
O'Neill, N. T., Dubovik, O., and Eck, T. F.: A modified Angstrom coefficient for the characterization of sub-micron aerosols, App. Opt., 40(14), 2368–2375, 2001.
O'Neill, N. T., Eck, T. F., Smirnov, A., Holben, B. N., and Thulasiraman, S.: Spectral discrimination of coarse and fine mode optical depth, J. Geophys. Res., 108, D17, 4559, doi:10.1029/2002JD002975, 2003.
Papanastasiou, D. K., Poupkou, A., Katragkou, E., Amiridis, V., Melas, D., Mihalopoulos, N., Basart, S., Pérez, C., and Baldasano, J. M.: An Assessment of the Efficiency of Dust Regional Modelling to Predict Saharan Dust Transport Episodes, Adv. Meteorol., 2010, 154368, doi:10.1155/2010/154368, 2010.
Papayannis, A., Amiridis, V., Mona, L., Tsaknakis, G., Balis, D., Bösenberg, J., Chaikovski, A., De Tomasi, F., Grigorov, I., and Mattis, I.: Systematic lidar observations of Saharan dust over Europe in the frame of EARLINET (2000–2002), J. Geophys. Res., 113, D10204, doi:10.1029/2007JD009028, 2008.
Pay, M. T., Piot, M., Jorba, O., Gassó, S., Gonçalves, M., Basart, S., Dabdub, D., Jiménez-Guerrero, P., and Baldasano, J. M.: A Full Year Evaluation of the CALIOPE-EU Air Quality Modeling System over Europe for 2004, Atmos. Environ., 44(27), 3322–3342, doi:10.1016/j.atmosenv.2010.05.040, 2010.
Pay, M. T., Jiménez-Guerrero, P., and Baldasano, J. M.: Implementation of resuspension from paved roads for the improvement of CALIOPE air quality system in Spain, Atmos. Environ.,

ACPD
11, 20575–20629, 2011

45, 802–807, doi:10.1016/j.atmosenv.2010.10.032, 2011.
Péré, J. C., Mallet, M., Pont, V., and Bessagnet, B.: Evaluation of an aerosol optical scheme in the chemistry-transport model CHIMERE, Atmos. Environ., 44, 3688–3699, doi:10.1016/j.atmosenv.2010.06.034, 2010.
Pérez, C., Nickovic, S., Baldasano, J. M., Sicard, M., Rocadenbosch, F., and Cachorro, V. E.: A long Saharan dust event over the western Mediterranean: Lidar, Sun photometer observations, and regional dust modeling, J. Geophys. Res., 111, D15214, doi:10.1029/2005JD006579, 2006a.
Pérez, C., Nickovic, S., Pejanovic, G., Baldasano, J. M., and Ozsoy, E.: Interactive dust-radiation modeling: A step to improve weather forecasts, J. Geophys. Res., 11, D16206, doi:10.1029/2005JD006717, 2006b.
Piot, M., Jorba, O., Jimenez, P., and Baldasano, J. M.: The Role of Lateral Boundary Conditions and Boundary Layer in Air Quality Modelling System, Eos Trans. AGU, 8, H212+, Abstract A41H-0212, 2008.
Pope, C. A. I., Ezzati, M., and Dockery, D. W.: Fine-Particulate Air Pollution and Life Expectancy in the United States, The New England Journal Med., 360, 376–386, 2009.
Putaud, J.-P., Van Dingenen, R., Mangoni, M., Virkkula, A., Raes, F., Maring, H., Prospero, J. M., Swietlicki, E., Berg, O. H., Hillamo, R., and Mäkelä, T.: Chemical mass closure and assessment of the origin of the submicron aerosol in the marine boundary layer and the free troposphere at Tenerife during ACE- 2, Tellus, 52B, 147–168, 2000.
Putaud, J.-P., Raes, F., Van Dingenen, R., Bruggemann, E., Facchini, M. C., Decesari, S., Fuzzi, S., Gehrig, R., Huglin, C., Laj, P., Lorbeer, G., Maenhaut, W., Mihalopoulos, N., Müller, K., Querol, X., Rodríguez, S., Schneider, J., Spindler, G., ten Brink, H., Torseth, K., and Wiedensohler, A.: European aerosol phenomenology 2: chemical characteristics of particulate matter at kerbside, urban, rural and background sites in Europe, Atmos. Environ., 38, 2579–2595, 2004.
Querol, X., Alastuey, A., Viana, M., Rodríguez, S., Artiano, B., Salvador, P., Santos, S. G. d., Patier, R. F., Ruiz, C. R., Rosae, J. d. l., Campa, A. S. d. l., Menendez, M., and Gilf, J. l.: Speciation and origin of PM10 and PM2.5 in Spain, Aerosol. Sci., 35, 1151–1172, doi:10.1016/j.jaerosci.2004.04.002, 2004.
Querol, X., Alastuey, A. Pey, J., Cusack, M., Pérez, N., Mihalopoulos, N., Theodosi, C., Gerasopoulos, E., Kubilay, N., and Koçak, M.: Variability in regional background aerosols within the Mediterranean, Atmos. Chem. Phys., 9, 4575–4591, doi:10.5194/acp-9-4575-

ACPD
11, 20575–20629, 2011

2009, 2009.
Remer, L. A., Kaufman, Y. J., Tanré, D., Mattoo, S., Chu, D. A., Martins, J. V., Li, R. R., Ichoku, C., Levy, R. C., Kleidman, R. G., Eck, T. F., Vermote, E. and Holben, B. N.: The MODIS Aerosol Algorithm, Products, and Validation, J. Atmos. Sci., 62, 947–973, 2005.
Rodríguez, S., Querol, X., Alastuey, A., Kallos, G., and Kakaliagou, O.: Saharan dust contributions to PM10 and TSP levels in Southern and Eastern Spain, Atmos. Environ., 35, 2433–2447, 2001.
Rodríguez, S., Alastuey, A., Alonso-Pérez, S., Querol, X., Cuevas, E., Abreu-Afonso, J., Viana, M., Pérez, N., Pandolfi, M., and de la Rosa, J.: Transport of desert dust mixed with North African industrial pollutants in the subtropical Saharan Air Layer, Atmos. Chem. Phys., 11, 6663-6685, doi:10.5194/acp-11-6663-2011, 2011.
Roy, B., Mathur, R., Gilliland, A. B., and Howard, S. C.: A comparison of CMAQ-based aerosol properties with IMPROVE, MODIS, and AERONET data, J. Geophys. Res, 112, D14301, doi:10.1029/2006JD008085, 2007.
Ryall, D. B., Derwent, R. G., Manning, A. J., Redington, A. L., Corden, J., Millington, W., Simmonds, P. G., O'Doherty, S., Carslaw, N., and Fuller, G. W.: The origin of high particulate concentrations over the United Kingdom, March 2000, Atmos. Environ., 36, 1363–1378, 2002.
Schaap, M., van Loon, M., ten Brink, H. M., Dentener, F. J., and Builtjes, P. J. H.: Secondary inorganic aerosol simulations for Europe with special attention to nitrate, Atmos. Chem. Phys., 4, 857–874, doi:10.5194/acp-4-857-2004, 2004.
Schell, B., Ackermann, I. J., Hass, H., Binkowski, F. S., and Ebel, A.: Modeling the formation of secondary organic aerosol within a comprehensive air quality model system, J. Geophys. Res., 106(D22), 28275–28293, doi:2001JD000384, 2001.
Seinfeld, J. H. and Pandis, S. N.: Atmospheric Chemistry and Physics: From Air Pollution to Climate Change, 1326 pp., John Wiley, New York, 1998.
Sicardi, V., Ortiz, J., Rincón, A., Jorba, O., Pay, M. T., Gassó, S., and Baldasano, J. M.: Ground-level ozone concentration over Spain: an application of Kalman Filter post-processing to reduce model uncertainties, Geoscientific Model Development Discussions, 4, 343–384, doi:10.5194/gmdd-4-343-2011, 2011.
Smirnov, A., Holben, B. N., Eck, T. F., Dubovik, O., and Slutsker, I.: Cloud screening and quality control algorithms for the AERONET database, Rem. Sens. Environ., 73, 337–349, 2000.
Szopa, S., Foret, G., Menut, L., and Cozic, A.: Impact of large scale circulation on Euro-

ACPD
11, 20575–20629, 2011

pean summer surface ozone and consequences for modelling forecast, Atmos. Environ., 43, 1189–1195, 2009.
Tang, I. N., Wong, W. T., and Munkelwitz, H. R.: The relative importance of atmospheric sulfates and nitrates in visibility reduction, Atmos. Environ., (1967), 15, 2463–2471, 1981.
Tegen, I. and Lacis, A. A.: Modeling of particle size distribution and its influence on the radiative properties of mineral dust aerosol, J. Geophys. Res., 101, 19237–19244, 1996.
Todd, M. C.: Quantifying uncertainty in estimates of mineral dust flux: An intercomparison of model performance over the Bodélé Depression, northern Chad, Geophys. Res, 113, D24107, doi:10.1029/2008JD010476, 2008.
Tombette, M., Chazette, P., Sportisse, B., and Roustan, Y.: Simulation of aerosol optical properties over Europe with a 3-D size-resolved aerosol model: comparisons with AERONET data, Atmos. Chem. Phys., 8, 7115–7132, doi:10.5194/acp-8-7115-2008, 2008.
Torseth, K. and Hov, O.: The EMEP Monitoring Strategy 2004–2009, Technical report 9/2003, EMEP/CCC, 2003.
Tsyro, S. G.: To what extent can aerosol water explain the discrepancy between model calculated and gravimetric PM_{10} and $PM_{2.5}$?, Atmos. Chem. Phys., 5, 515–532, doi:10.5194/acp-5-515-2005, 2005.
Tsyro, S., Simpson, D., Tarrasón, L., Klimont, Z., Kupiainen, K., Pio, C., and Yttri, K. E.: Modeling of elemental carbon over Europe, J. Geophys. Res., 112, D23S19, doi:10.1029/2006JD008164, 2007.
U.S. EPA.: Interim Procedures for Evaluating Air Quality Models (Revised), Technical Report, EPA-450/4-91-013, U.S. Environmental Protection Agency, Office of Air Quality Planning and Standards, Research Triangle Park, NC, 1984
U.S. EPA.: Guideline for Regulatory Application of the Urban Airshed Model, Technical Report. EPA-450/4-91-013, U.S. Environmental Protection Agency, Office of Air Quality Planning and Standards, Research Triangle Park, NC, 1991.
Volkamer, R., Jiménez, J. L., San Martini, F., Dzepina, K., Zhang, Q., Salcedo, D., Molina, L. T., Worsnop, D .R., and Molina, M. J.: Secondary organic aerosol formation from anthropogenic air pollution: Rapid and higher than expected, J. Geophys. Res. Lett., 33, L17811, doi:10.1029/2006GL026899, 2006.
Weil, J. C., Sykes, R. I., and Venkatram, A.: Evaluating air-quality models: review and outlook, Appl. Meteo., 31, 1121–1145, 1992.
WHO: WHO air quality guidelines global update 2005, Bonn, Germany, World Health Organi-

ACPD
11, 20575–20629, 2011

zation, 2005.
Wyat Appel, K., Gilliland, A. B., Sarwar, G., and Gilliam, R. C.: Evaluation of the Community Multiscale Air Quality (CMAQ) model version 4.5: Sensitivities impacting model performance: Part I–Ozone, Atmos. Environ., 41, 9603–9615, 2007.
Wyat Appel, K., Bhave, P. V., Gilliland, A. B., Sarwar, G., and Roselle, S. J.: Evaluation of the community multiscale air quality (CMAQ) model version 4.5: Sensitivities impacting model performance; Part II particulate matter, Atmos. Environ., 6057–6066, doi:10.1016/j.atmosenv.2008.03.036, 2008.
Yttri, K. E. and Aas, W.: Transboundary Particulate Matter in Europe: Status Report 2006, EMEP Report, 2006.
Zhang, K., Knipping, E., Wexler, A., Bhave, P., and Tonnesen, G.: Size distribution of sea-salt emissions as a function of relative humidity, Atmos. Environ., 39, 3373–3379, 2005.

ACPD
11, 20575–20629, 2011

Table 1. Seasonal and annual statistics obtained with CALIOPE over Europe for 2004 at the EMEP/CREATE stations for SIA (i.e. sulphate, nitrate, and ammonium) and SSA (i.e. chloride and sodium). Winter: January, February and December; Spring: March, April, May; Summer: June, July, August; Autumn: September, October, November. The number of data points indicates the number of pair measurement-model used to compute the statistics. The calculated statistics are: measured mean for available data, modelled mean for the whole year, correlation (r), Mean Bias (MB), Mean Normalize Bias Error (MNBE), Root Mean Square Error (RMSE), Mean Fractional Bias (MFB) and Mean Fractional Error (MFE).

		Data Points	Obs. Mean	Mod. mean	*r*	MB	MNBE(%)	RMSE	MFB(%)	MFE(%)
PM2.5 daily (16 stations)	Annual	5118	12.3	5.7	0.47	−6.30	−45.0	11.2	−72	80
	Winter	1171	12.2	4.8	0.62	−8.40	−47.0	15.3	−78	86
	Spring	1264	12.2	5.2	0.50	−6.70	−50.0	10.6	−79	84
	Summer	1396	11.5	6.8	0.49	−5.40	−45.0	9.1	−71	78
	Autumn	1287	12.3	6.2	0.52	−5.00	−39.0	9.3	−62	72
PM10 daily (25 stations)	Annual	8389	17.8	7.5	0.57	−10.30	−50.0	15.8	−79	84
	Winter	1994	18.0	6.6	0.54	−11.20	−47.0	18.2	−78	86
	Spring	2087	17.7	7.1	0.54	−10.50	−54.0	15.0	−84	87
	Summer	2204	18.5	8.2	0.60	−10.50	−54.0	16.1	−83	86
	Autumn	2104	17.0	8.1	0.62	−9.00	−44.0	13.5	−70	77
Sulfate daily (53 stations)	Annual	18227	1.7	1.4	0.49	−0.30	33.6	1.3	−8	55
	Winter	4524	1.5	1.0	0.30	−0.50	11.6	1.6	−24	65
	Spring	4675	1.8	1.4	0.50	−0.50	15.2	1.4	−19	54
	Summer	4598	1.8	1.7	0.59	−0.10	52.7	1.2	7	47
	Autumn	4430	1.6	1.5	0.58	−0.10	55.5	1.2	4	55
Nitrate daily (31 stations)	Annual	8968	2.0	1.0	0.58	−1.00	−9.7	2.3	−87	113
	Winter	2208	2.7	1.4	0.60	−1.10	21.6	3.1	−68	99
	Spring	2264	2.3	1.1	0.56	−1.10	−6.5	2.6	−76	104
	Summer	2252	1.2	0.4	0.29	−0.80	−55.6	1.3	−121	133
	Autumn	2244	1.8	0.9	0.53	−0.80	2.4	2.0	−84	115
Ammonium daily (19 stations)	Annual	4944	1.2	0.8	0.62	−0.50	32.8	1.2	−32	72
	Winter	1239	1.4	0.7	0.70	−0.80	28.2	1.5	−42	80
	Spring	1300	1.5	0.8	0.62	−0.60	23.1	1.3	−37	73
	Summer	1205	1.0	0.7	0.48	−0.20	38.9	0.8	−22	63
	Autumn	1200	1.1	0.8	0.64	−0.30	42.1	0.9	−24	70
Chloride daily (5 stations)	Annual	1434	0.3	0.3	0.46	0.00	413.9	0.5	49	106
	Winter	355	0.4	0.3	0.44	−0.10	297.5	0.6	14	97
	Spring	368	0.3	0.3	0.38	0.00	308.7	0.7	39	104
	Summer	362	0.1	0.3	0.53	0.10	598.2	0.3	78	115
	Autumn	349	0.3	0.4	0.64	0.10	451.9	0.5	65	109
Sodium daily (9 stations)	Annual	3204	0.7	1.2	0.67	0.50	176.1	1.6	16	77
	Winter	794	0.9	1.5	0.70	0.60	176.3	1.9	18	81
	Spring	806	0.7	1.1	0.64	0.50	176.6	1.6	10	79
	Summer	805	0.6	0.9	0.67	0.30	128.3	1.1	11	72
	Autumn	799	0.8	1.4	0.65	0.70	223.7	1.8	26	77

ACPD
11, 20575–20629, 2011

Table 2. Seasonal and annual statistics obtained with CALIOPE over Europe for 2004 at the AERONET stations for AOD, AOD_{fine} and AOD_{coarse}. Winter: January, February and December; Spring: March, April, May; Summer: June, July, August; Autumn: September, October, November. The number of data points indicates the number of pair measurement-model used to compute the statistics. The calculated statistics are: measured mean for available data, modelled mean for the whole year, correlation (r), Mean Bias (MB), Mean Normalize Bias Error (MNBE), Root Mean Square Error (RMSE), Mean Fractional Bias (MFB) and Mean Fractional Error (MFE).

		Data Points	Obs. Mean	Mod. mean	r	MB	MNBE(%)	RMSE	MFB(%)	MFE(%)
AOD hourly (35 stations)	Annual	34925	0.18	0.10	0.51	−0.07	−31.0	0.15	−53	66
	Winter	4175	0.12	0.07	0.36	−0.05	−23.1	0.13	−49	69
	Spring	9099	0.19	0.11	0.49	−0.07	−32.3	0.16	−57	70
	Summer	14249	0.19	0.11	0.49	−0.08	−34.8	0.16	−56	66
	Autumn	7402	0.16	0.10	0.62	−0.06	−26.6	0.13	−45	58
AOD_{fine} hourly (16 stations)	Annual	15914	0.22	0.10	0.52	−0.13	−48.7	0.19	−75	80
	Winter	1459	0.14	0.06	0.42	−0.09	−45.9	0.16	−78	87
	Spring	3828	0.24	0.11	0.55	−0.13	−49.5	0.19	−77	82
	Summer	7250	0.24	0.10	0.45	−0.14	−50.7	0.20	−77	80
	Autumn	3377	0.21	0.10	0.62	−0.12	−44.9	0.19	−69	74
AOD_{coarse} hourly (16 stations)	Annual	15914	0.06	0.02	0.63	−0.04	−72.9	0.07	−134	139
	Winter	1459	0.05	0.02	0.25	−0.04	−69.4	0.07	−133	141
	Spring	3828	0.07	0.02	0.58	−0.04	−73.3	0.09	−137	142
	Summer	7250	0.05	0.02	0.70	−0.03	−73.1	0.06	−135	139
	Autumn	3377	0.06	0.02	0.71	−0.04	−73.6	0.07	−130	133
AOD daily (35 stations)	Annual	4920	0.18	0.11	0.56	−0.07	−28.2	0.14	−47	60
	Winter	792	0.12	0.07	0.41	−0.05	−23.6	0.12	−46	63
	Spring	1267	0.19	0.12	0.52	−0.07	−28.8	0.15	−51	64
	Summer	1689	0.20	0.12	0.55	−0.08	−33.3	0.15	−51	60
	Autumn	1172	0.16	0.11	0.67	−0.06	−24.5	0.12	−39	52
AOD_{fine} daily (16 stations)	Annual	2318	0.22	0.10	0.59	−0.12	−45.1	0.18	−69	74
	Winter	304	0.14	0.06	0.45	−0.08	−43.8	0.14	−71	80
	Spring	556	0.25	0.12	0.58	−0.13	−45.9	0.18	−70	75
	Summer	919	0.24	0.10	0.53	−0.14	−47.5	0.19	−70	73
	Autumn	539	0.21	0.10	0.68	−0.11	−41.0	0.19	−62	69
AOD_{coarse} daily (16 stations)	Annual	2318	0.06	0.02	0.70	−0.04	−74.6	0.07	−134	−138
	Winter	304	0.05	0.01	0.24	−0.04	−71.0	0.07	−132	138
	Spring	556	0.07	0.02	0.65	−0.05	−72.7	0.08	−134	138
	Summer	919	0.05	0.02	0.77	−0.03	−76.9	0.06	−139	141
	Autumn	539	0.06	0.02	0.80	−0.04	−74.6	0.06	−130	131

ACPD
11, 20575–20629, 2011

Table 3. Seasonal and annual multiplicative correction factors to SIA (sulphates, nitrates and ammonium) and EC + OC obtained minimizing a weighted sum of the squared difference between the modelled and measured chemical aerosol surface concentrations on total fraction mass on a daily basis over Europe for 2004. Winter: January, February and December; Spring: March, April, May; Summer: June, July, August; Autumn: September, October, November.

	Sulphates	Nitrates	Ammonium	OC + EC
Winter	1.7	1.7	2.0	4
Spring	1.4	1.8	1.7	4
Summer	1.2	1.9	1.4	4
Autumn	1.1	1.5	1.2	4
Annual	1.3	1.7	1.6	4

ACPD
11, 20575–20629, 2011

Table 4. Seasonal and annual statistics obtained with CALIOPE and the seasonal correction factors applied to sulphates, nitrates, ammonium and EC + OC over Europe for 2004 at the EMEP stations for PM2.5 and PM10 and at the AERONET stations for AOD_{fine} and AOD. Winter: January, February and December; Spring: March, April, May; Summer: June, July, August; Autumn: September, October, November. The number of data points indicates the number of pair measurement-model used to compute the statistics. The calculated statistics are: measured mean for available data, modelled mean for the whole year, correlation (r), Mean Bias (MB), Mean Normalize Bias Error (MNBE), Root Mean Square Error (RMSE), Mean Fractional Bias (MFB) and Mean Fractional Error (MFE).

		Data Points	Obs. Mean	Mod. mean	r	MB	MNBE(%)	RMSE	MFB(%)	MFE(%)
PM2.5 daily (16 stations)	Annual	5118	12.30	10.02	0.61	−2.31	−6.2	8.89	−22	47
	Winter	1171	12.20	10.38	0.67	−3.26	−3.2	11.72	−18	55
	Spring	1264	12.20	9.83	0.59	−2.34	−12.3	8.36	−33	45
	Summer	1396	11.50	9.95	0.55	−2.21	−13.2	7.54	−28	45
	Autumn	1287	12.30	9.94	0.62	−1.51	4.8	7.71	−19	45
PM10 daily (25 stations)	Annual	8389	17.80	11.65	0.62	−6.16	−20.7	12.91	−38	54
	Winter	1994	18.00	11.85	0.65	−6.15	−15.3	14.15	−32	57
	Spring	2087	17.70	11.97	0.59	−5.70	−24.6	15.15	−38	51
	Summer	2204	18.50	11.19	0.60	−7.35	−30.6	16.15	−48	56
	Autumn	2104	17.00	11.62	0.66	−5.38	−11.5	17.15	−35	52
AOD_{fine} hourly (16 stations)	Annual	15914	0.22	0.15	0.55	−0.07	6.3	0.16	−36	6
	Winter	1459	0.14	0.10	0.56	−0.05	15.5	0.13	−26	55
	Spring	3828	0.24	0.18	0.57	−0.06	2.3	0.16	−32	50
	Summer	7250	0.24	0.15	0.48	−0.08	1.6	0.16	−35	50
	Autumn	3377	0.21	0.14	0.66	−0.08	15.2	0.16	−36	52
AOD hourly (35 stations)	Annual	34925	0.18	0.15	0.56	−0.02	−16.5	0.13	−12	46
	Winter	4175	0.12	0.11	0.48	−0.00	−13.4	0.01	1	49
	Spring	9099	0.19	0.18	0.55	−0.01	−19.7	0.14	−12	45
	Summer	14249	0.19	0.16	0.53	−0.04	−18.5	0.14	−16	45
	Autumn	7402	0.16	0.14	0.66	−0.03	−10.0	0.12	−13	46
AOD_{fine} daily (16 stations)	Annual	2318	0.22	0.16	0.61	−0.07	−13.3	0.15	−28	46
	Winter	304	0.14	0.11	0.54	−0.03	0.0	0.12	−19	48
	Spring	556	0.25	0.19	0.60	−0.06	−11.9	0.15	−25	44
	Summer	919	0.24	0.16	0.56	−0.08	17.1	0.16	−30	46
	Autumn	539	0.21	0.14	0.71	−0.07	−16.1	0.16	−31	48
AOD daily (35 stations)	Annual	4920	0.18	0.14	0.60	−0.04	−1.9	0.12	−15	42
	Winter	792	0.12	0.11	0.57	−0.01	−14.4	0.10	−3	43
	Spring	1267	0.19	0.17	0.55	−0.02	−3.1	0.12	−16	40
	Summer	1689	0.20	0.15	0.59	−0.05	−7.4	0.12	−20	43
	Autumn	1172	0.16	0.13	0.70	−0.03	−3.8	0.11	−18	44

ACPD
11, 20575–20629, 2011

Table A1. Coordinates, altitude and the chemical species measured of the 54 selected EMEP 5 stations are included. The code is composed by 2-letter country code plus 2-digit station code. Zone of location is defined in Fig. 1.

Station Name	Code	Zone	Lat.(°/N)	Lon.(°/E)	Alt.(m)	Network	Na^+	Cl^-	SO_4^{-2}	NO_3^-	NH_4^+	OC	EC
Anholt	DK08	Nord	56.717	11.517	40	EMEP	x		x				
Barcarrota	ES11	W.IP	38.476	−6.923	393	EMEP			x	x			
Birkenes	NO01	Nord	58.383	8.250	190	EMEP/CREATE	x	x	x	x	x	x	x
Cabo de Creus	ES10	E.IP-W.Med	42.319	3.317	23	EMEP			x	x			
Campisábalos	ES09	W.IP	41.281	−3.143	1360	EMEP			x	x			
Chopok	SK02	E.Eu	48.933	19.583	2008	EMEP			x				
Deuselbach	DE04	NW.Eu	49.767	7.050	480	EMEP			x				
Diabla Gora	PL05	E.Eu	54.150	22.067	157	EMEP			x				
Donon	FR08	C.Eu	48.500	7.133	775	EMEP			x				
Els Torms	ES14	E.IP-W.Med	41.400	0.717	470	EMEP			x	x			
Eskdalemuir	GB02	NW.Eu	55.313	−3.204	243	EMEP			x				
High Muffles	GB14	NW.Eu	54.334	−0.808	267	EMEP			x				
Illmitz	AT02	E.Eu	47.767	16.767	117	EMEP	x		x	x	x		
Iraty	FR12	S.Fr	43.033	−1.083	1300	EMEP			x				
Iskrba	SI08	N.It	45.567	14.867	520	EMEP	x	x	x				
Ispra	IT04	N.It	45.800	8.633	209	EMEP			x	x	x		
Jarczew	PL02	E.Eu	51.817	21.983	180	EMEP			x	x	x		
Jungfraujoch	CH01	C.Eu	46.550	7.983	3573	EMEP		x	x	x	x		
Kollumerwaard	NL09	NW.Eu	53.334	6.277	1	EMEP				x	x		
Kosetice	CZ03	E.Eu	49.583	15.083	534	EMEP			x				
K-puszta	HU02	E.Eu	46.967	19.583	125	EMEP			x	x	x		
La Tardière	FR15	C.Fr	46.650	0.750	746	EMEP			x				
Le Casset	FR16	C.Eu	45.000	6.467	746	EMEP			x				
Leba	PL04	Nord	54.750	17.533	2	EMEP			x	x	x		
Liesek	SK05	E.Eu	49.367	19.683	892	EMEP			x	x			
Lough Navar	GB06	N.Atl	54.443	−7.870	126	EMEP			x				
Melpitz	DE44	NW.Eu	52.53	12.93	86	CREATE	x	x	x	x	x	x	x
Montandon	FR14	C.Eu	47.183	6.500	746	EMEP			x				
Montelibretti	IT01	C.Med	42.100	12.633	48	EMEP			x	x	x		
Morvan	FR10	C.Fr	47.267	4.083	620	EMEP			x				
Niembro	ES08	W.IP	43.442	−4.850	134	EMEP			x	x			
O Savñao	ES16	W.IP	42.653	−7.705	506	EMEP			x	x			
Payerne	CH02	C.Eu	46.817	6.950	510	EMEP			x				
Penausende	ES13	W.IP	41.283	-5.867	985	EMEP			x	x			
Peyrusse Vieille	FR13	S.Fr	43.375	0.104	236	EMEP			x				
Preila	LT15	Nord	55.350	21.067	5	EMEP			x				
Råö	SE14	Nord	57.400	11.917	5	EMEP			x				
Revin	FR09	NW.Eu	49.900	4.633	390	EMEP			x				
Rigi	CH05	C.Eu	47.069	8.466	1030	EMEP			x				
Risco Llamo	ES15	W.IP	39.517	−4.350	1241	EMEP			x	x			
Rucava	LV10	Nord	56.217	21.217	5	EMEP			x	x	x		
Skreådalen	NO08	Nord	58.817	6.717	475	EMEP	x	x	x	x	x		
Sniezka	PL03	E.Eu	50.733	15.733	1603	EMEP			x	x	x		
Starina	SK06	E.Eu	49.050	22.267	345	EMEP			x	x			
Svratouch	CZ01	E.Eu	49.733	16.033	737	EMEP			x				
Tange	DK03	Nord	56.350	9.600	13	EMEP	x		x				
Topolniky	SK07	E.Eu	47.960	17.861	113	EMEP			x	x			
Utö	FI09	Nord	59.779	21.377	7	EMEP	x		x		x		
Valentina Observatory	IE01	N.Atl	51.940	−10.244	11	EMEP	x		x				
Vavihill	SE11	Nord	56.017	13.150	175	EMEP			x				
Víznar	ES07	E.IP-W.Med	37.233	−3.533	1265	EMEP			x	x			
Yarner Wood	GB13	NW.Eu	50.596	−3.713	119	EMEP			x				
Zarra	ES12	E.IP-W.Med	39.086	−1.102	885	EMEP			x	x			
Zoseni	LV16	Nord	57.133	25.917	183	EMEP			x	x	x		

ACPD
11, 20575–20629, 2011

Table A2. Zone of location of the 35 AERONET stations which is defined in Fig. 1; class of location which is defined as stations: in remote (R), urban (U) or sub-rural (S) areas and in littoral localizations (C); coordinates, altitude, the number of measurements (Dataset), the number of hours (Hr.), the number of days (Dy.) and months (Mo.), the percentage of cloud screened data (F) in the observation periods of the 35 selected AERONET stations and the availability of the quality-assured SDA retrieval products (SDA).

Station name	Code	Zone	Class	Lon.(°/E)	Lat.(°/N)	Alt.(m)	First date	Last date	N	Hr.	Dy.	Mo.	F(%)	SDA
Avignon	AVI	E.IP-W.Med	U	4.88	43.93	32	01/01/2004	31/12/2004	7131	1998	264	12	34.52	
Barcelona	BCN	E.IP-W.Med	U/C	2.12	41.39	125	16/12/2004	31/12/2004	201	59	11	1	39.12	
Belsk	BEL	E.Eu	R	20.79	51.84	190	10/02/2004	11/12/2004	3173	1039	150	10	41.49	x
Blida	BLI	E.IP-W.Med	S/C	2.88	36.51	230	01/01/2004	27/12/2004	4598	1368	220	12	33.55	x
Cabo da Roca	ROC	W.IP	R/C	−9.50	38.78	140	04/01/2004	14/10/2004	4179	1259	193	10	39.17	
Carpentras	CAR	E.IP-W.Med	R	5.06	44.08	100	02/01/2004	15/11/2004	6905	1979	242	11	37.12	x
Dunkerque	DUN	NW.EU	U/C	2.37	51.04	0	20/07/2004	06/12/2004	871	331	65	6	56.17	
El Arenosillo	ARE	W.IP	R/C	−6.73	37.11	0	01/01/2004	31/12/2004	9235	2437	302	12	23.70	
ETNA	ETN	C.Med	U/C	15.02	37.61	736	01/01/2004	15/04/2004	871	226	40	3	39.25	x
Evora	EVO	W.IP	U	−7.91	38.57	293	02/01/2004	31/12/2004	7860	2205	266	12	29.75	
Fontainebleau	FON	NW.EU	R	2.68	48.41	85	28/03/2004	30/11/2004	1411	568	106	9	53.65	x
Forth Crete	CRE	E.Med	S/C	25,28	35,33	20	01/01/2004	31/12/2004	9634	2352	272	12	24.90	x
Hamburg	HAM	NW.EU	U	9.97	53.57	105	18/01/2004	29/12/2004	2094	691	115	11	46.59	x
Helgoland	HEL	NW.EU	R/C	7.89	54.18	33	28/04/2004	21/10/2004	470	202	40	7	40.42	x
IFT-Leipzig	LEI	C.Eu	U	12.44	51.35	125	08/01/2004	21/12/2004	1567	642	129	12	49.15	x
ISDGM CNR	CNR	N.It	R/C	12.33	45.44	20	01/01/2004	08/11/2004	5029	1566	209	11	48.26	x
Ispra	ISP	N.It	S	8.63	45.80	235	01/01/2004	31/12/2004	3942	1301	200	12	44.50	x
Laegeren	LAE	C.Eu	R	8.35	47.48	735	30/03/2004	25/12/2004	2694	848	125	10	41.24	x
Lampedusa	LAM	C.Med	R/C	12.63	35.52	45	01/01/2004	30/12/2004	2561	848	139	8	30.63	
Le Fauga	FAU	S.Fr	R	1.28	43.38	193	04/01/2004	22/12/2004	3736	1131	176	11	40.73	
Lecce University	LEC	C.Med	R	18.11	40.34	30	01/01/2004	07/10/2004	5489	1671	219	10	34.28	x
Lille	LIL	NW.EU	U	3.14	50.61	60	03/01/2004	29/12/2004	943	346	71	8	51.99	
Mainz	MAI	C.Eu	S	8.30	50.00	150	09/01/2004	30/11/2004	3191	1058	172	11	48.94	x
Modena	MOD	N.It	U	10.95	44.63	56	15/03/2004	24/06/2004	1899	554	70	4	41.35	
Munich Maisach	MUN	C.Eu	R	11.26	48.21	520	22/03/2004	09/06/2004	153	74	18	4	48.35	x
Nicelli Airport	NIC	N.It	S/C	12.38	45.43	13	25/08/2004	06/09/2004	389	94	10	2	27.45	
Palaiseau	PLS	NW.EU	S	2.21	48.70	156	30/03/2004	29/12/2004	2725	889	139	10	45.08	
Palencia	PAL	W.IP	U	−4.52	41.99	750	21/01/2004	30/12/2004	7389	2010	265	12	32.69	
Paris	PAR	NW.EU	U	2.33	48.87	50	24/11/2004	28/12/2004	106	34	7	2	38.59	
Rome Tor Vergata	ROM	C.Med	R	12.65	41.84	130	01/01/2004	31/12/2004	2256	601	106	8	40.05	
SMHI	SMH	Nord	U	16.15	58.58	0	02/06/2004	08/07/2004	493	182	25	2	34.73	x
The Hague	HAG	NW.EU	S/C	4.33	52.11	18	21/03/2004	21/11/2004	1376	476	73	7	49.67	
Toulon	TUL	E.IP-W.Med	U/C	6.01	43.14	50	15/11/2004	31/12/2004	430	128	24	2	42.09	
Venise	VEN	N.It	R/C	12.51	45.31	10	01/01/2004	30/12/2004	10257	1872	230	12	36.34	
Villefranche	VIL	E.IP-W.Med	S/C	7.33	43.68	130	07/01/2004	10/11/2004	7120	1936	235	11	32.81	

ACPD
11, 20575–20629, 2011

Table B1. Definitions of the statistics used in the study. $(o_i)i$ and $(c_i)i$ are the observed and the modelled concentrations at time and location i, respectively. n: the number of data.

Statistic Parameter	Formula
Correlation coefficient (r)	$r = \frac{\sum_{i=1}^{n}(c_i-\overline{c})\cdot(o_i-\overline{o})}{\sqrt{\sum_{i=1}^{n}(c_i-\overline{c})^2}\cdot\sqrt{\sum_{i=1}^{N}(o_i-\overline{o})^2}}$
Mean Bias (MB)	$\mathrm{MB} = \frac{1}{n}\sum_{i=1}^{n}(c_i - o_i)$
Root Mean Square Error (RMSE)	$\mathrm{RMSE} = \sqrt{\frac{1}{n}\sum_{i=1}^{n}(c_i - o_i)^2}$
Mean Normalized Bias Error (MNBE)	$\mathrm{MNBE} = \sum_{i=1}^{n}\frac{(c_i-o_i)}{o_i}\cdot 100\%$
Mean Fractionalized Bias (MFB)	$\mathrm{MFB} = \frac{1}{n}\sum_{i=1}^{n}\frac{(c_i-o_i)}{o_i}\cdot 100\%$
Mean Fractionalized Error (MFE)	$\mathrm{MFE} = \frac{1}{n}\sum_{i=1}^{n}\frac{(c_i-o_i)}{\left(\frac{c_i+o_i}{2}\right)}\cdot 100\%$

ACPD
11, 20575–20629, 2011

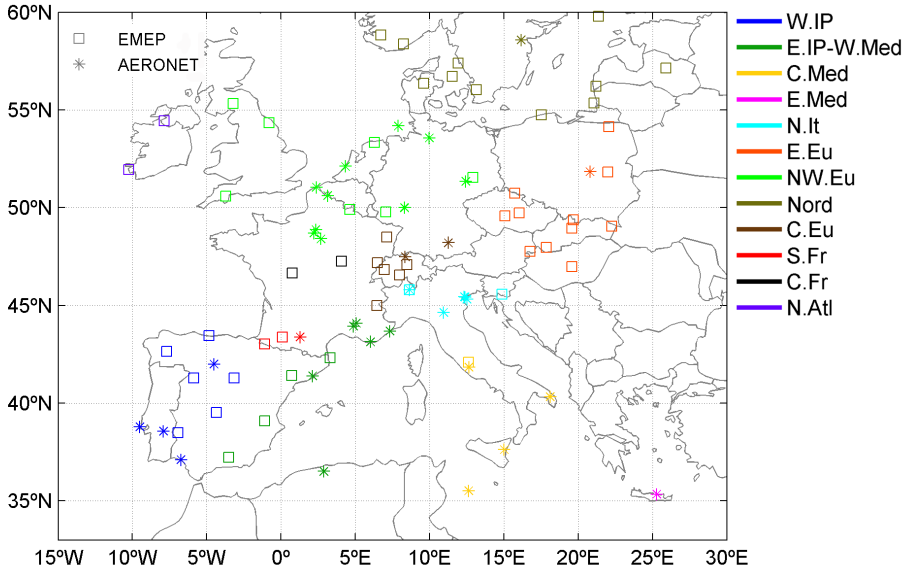

Fig. 1. Study domain and spatial distribution of 54 selected EMEP stations (indicated by square marks) and 35 selected AERONET stations (indicated by star marks) over the study domain. The different colours indicate the different regions which are defined as: Western Iberian Peninsula (W.IP); Eastern Iberian Peninsula-Western Mediterranean (E.IP-W.Med), Central Mediterranean (C.Med), Eastern Mediterranean (E.Med), North of Italy (N. It.), Eastern Europe (E.Eu), Northwestern Europe (NW.Eu), Southern France (S.Fr.), Central Europe (C.Eu), Nordic (Nord), Central France (C.Fr) and North Atlantic (N.Atl).

ACPD
11, 20575–20629, 2011

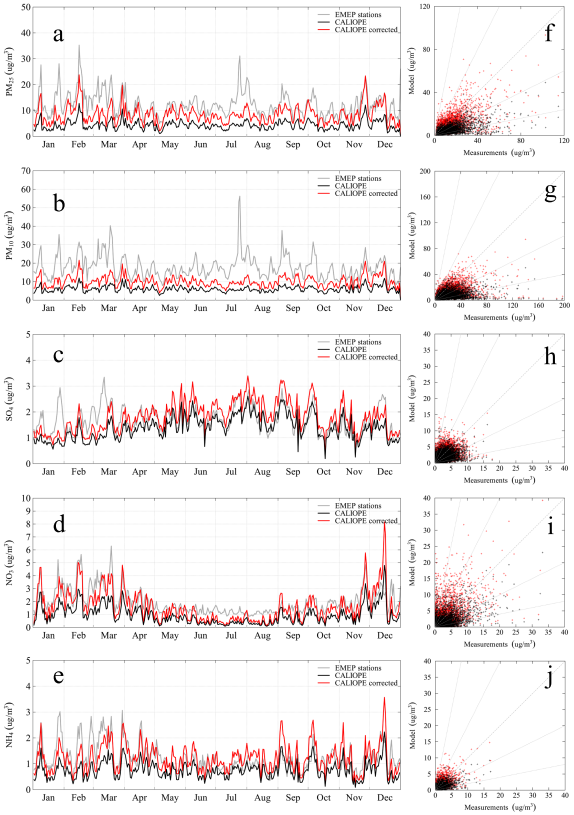

Fig. 2. Modelled (black lines), corrected-modelled (red lines) and measured (grey lines) time series (right) and scatter plots (left) of daily mean concentrations for PM2.5, PM10, sulphates, nitrates and ammonium at the EMEP/CREATE stations, respectively. The scatter plots include the 1:1, 1:2, 2:1, 1:5 and 5:1 reference lines.

ACPD
11, 20575–20629, 2011

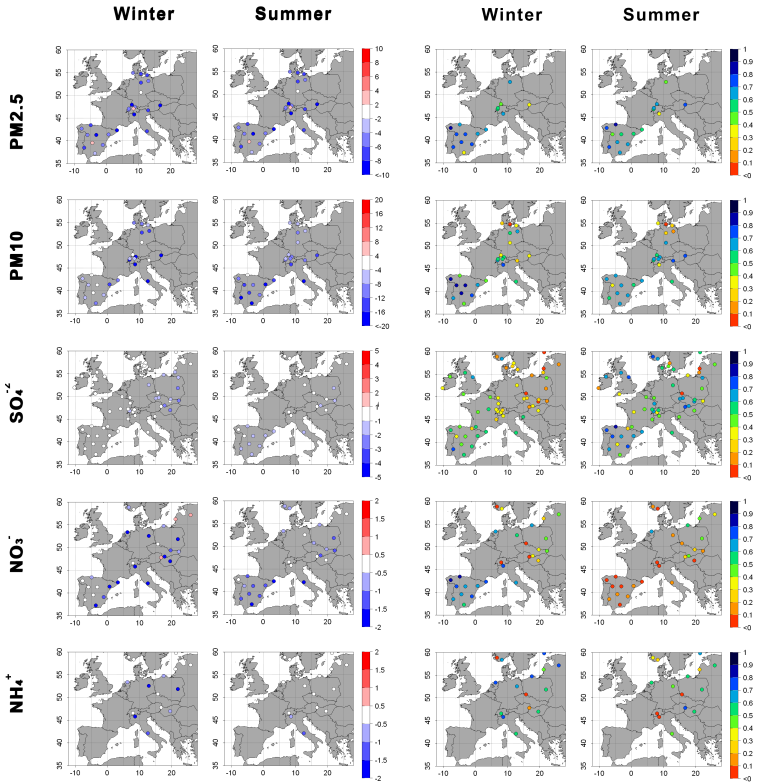

Fig. 3. Spatial distribution of mean bias (left panels) and the correlation coefficient (right panels) at all stations for PM2.5, PM10, sulphates (SO_4^{-2}), nitrates (NO_3^-) and ammonium (NH_4^+). The four columns represent the winter and summer seasons for 2004, respectively for each parameter.

ACPD
11, 20575–20629, 2011

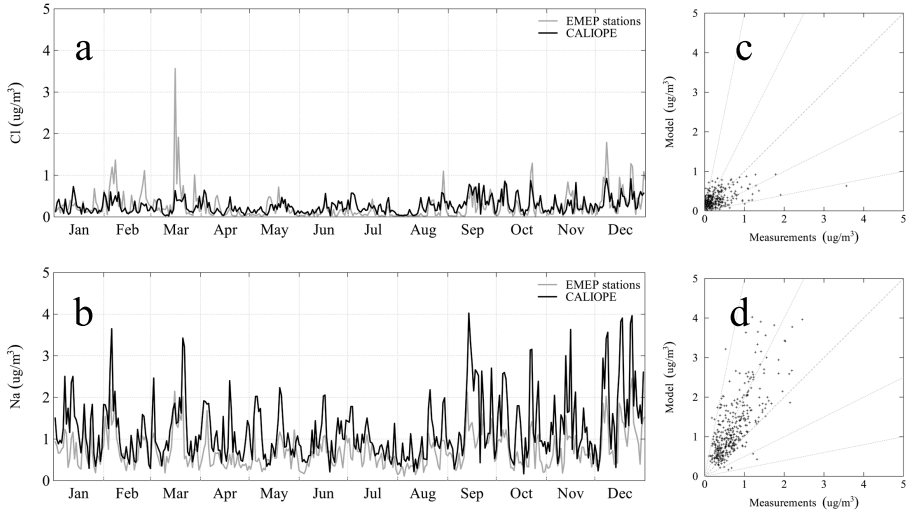

Fig. 4. Modelled (black lines) and measured (grey lines) time series (left) and scatter plots (right) of daily mean concentrations for sea salt chemical species (i.e. chlorine and sodium), at the EMEP/CREATE stations, respectively. The scatter plots include the 1:1, 1:2, 2:1, 1:5 and 5:1 reference lines.

ACPD
11, 20575–20629, 2011

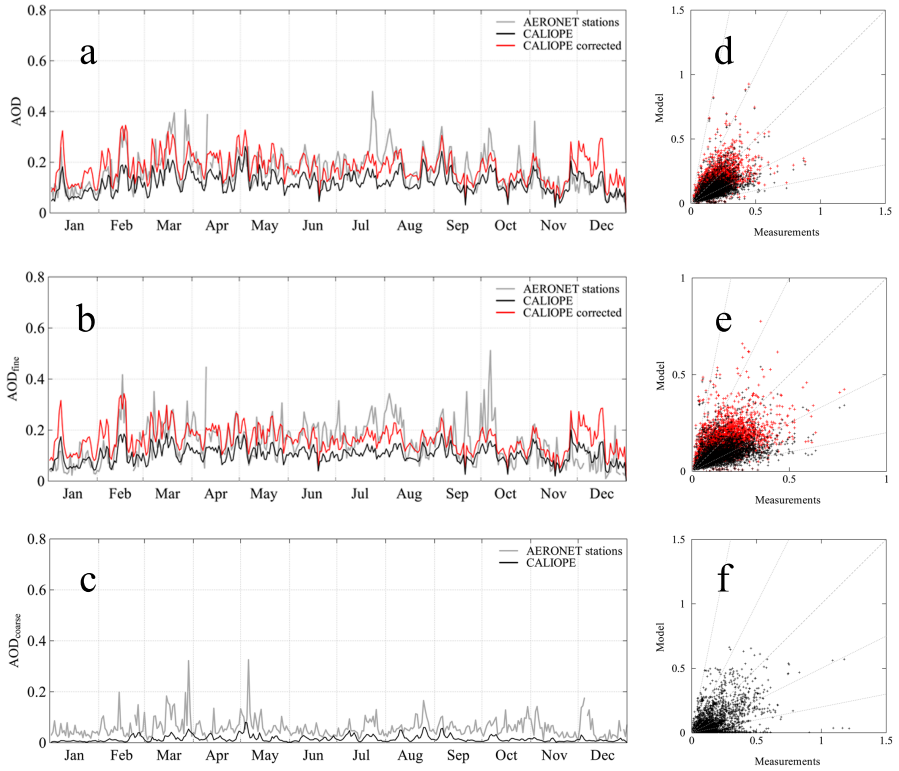

Fig. 5. Modelled (black lines), corrected-modelled (red lines) and measured (grey lines) time series (right) in daily mean concentrations and scatter plots (left) in hourly mean concentration values for AOD, AOD_{fine} and AOD_{coarse} at the AERONET stations, respectively. The scatter plots include the 1:1, 1:2, 2:1, 1:5 and 5:1 reference lines.

ACPD
11, 20575–20629, 2011

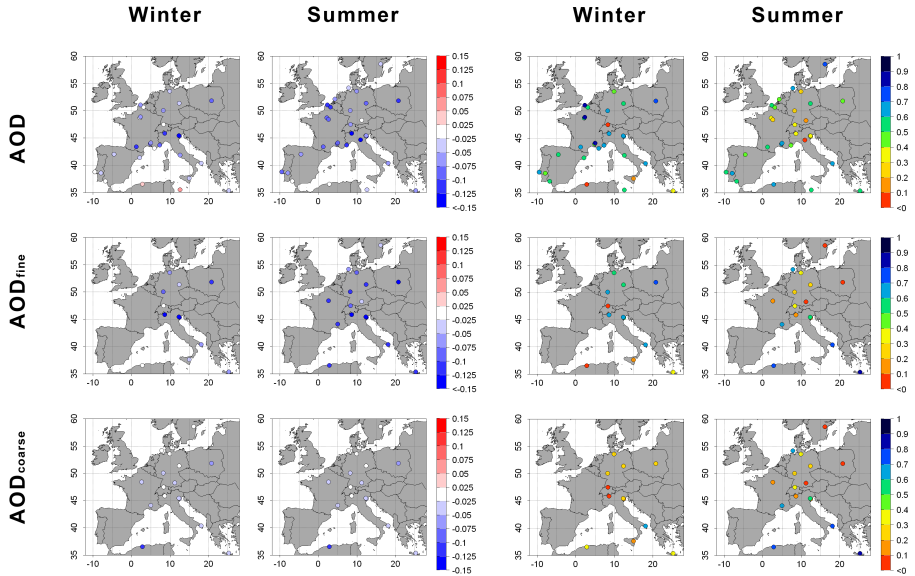

Fig. 6. Spatial distribution of mean bias (left panels) and the correlation coefficient (right panels) at all stations for AOD, AOD_{fine} and AOD_{coarse} in hourly basis. The four columns represent the winter and summer seasons for 2004, respectively for each parameter.

ACPD
11, 20575–20629, 2011

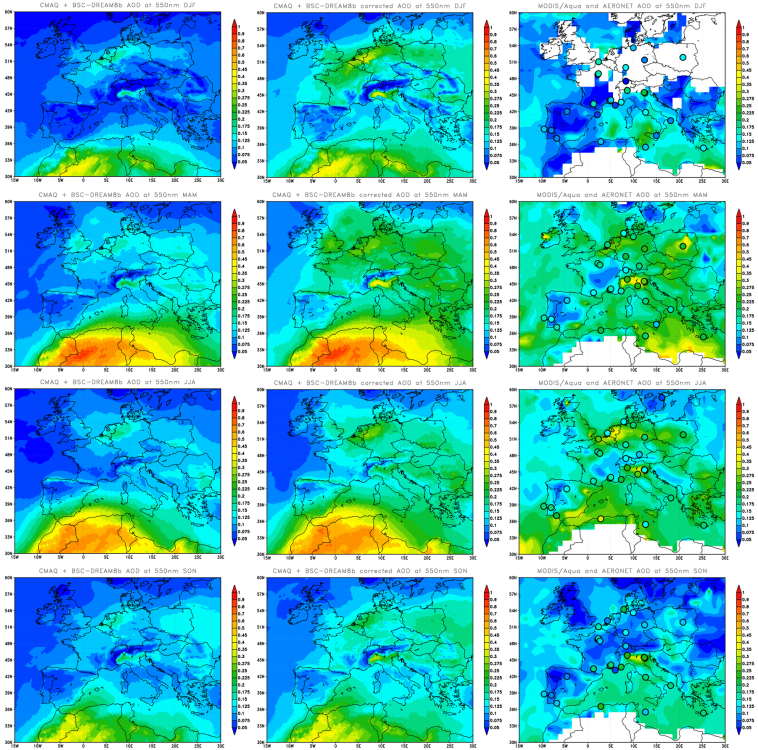

Fig. 7. Seasonal AOD average (from the top to bottom panels) of CMAQ + BSC-DREAM8b without correction factor (left panels), CMAQ + BSC-DREAM8b with correction factors for sulphates, nitrates ammonium and EC + OC (central panels) and MODIS/Aqua AOD product as well AERONET seasonal mean values (colour points).

ACPD
11, 20575–20629, 2011

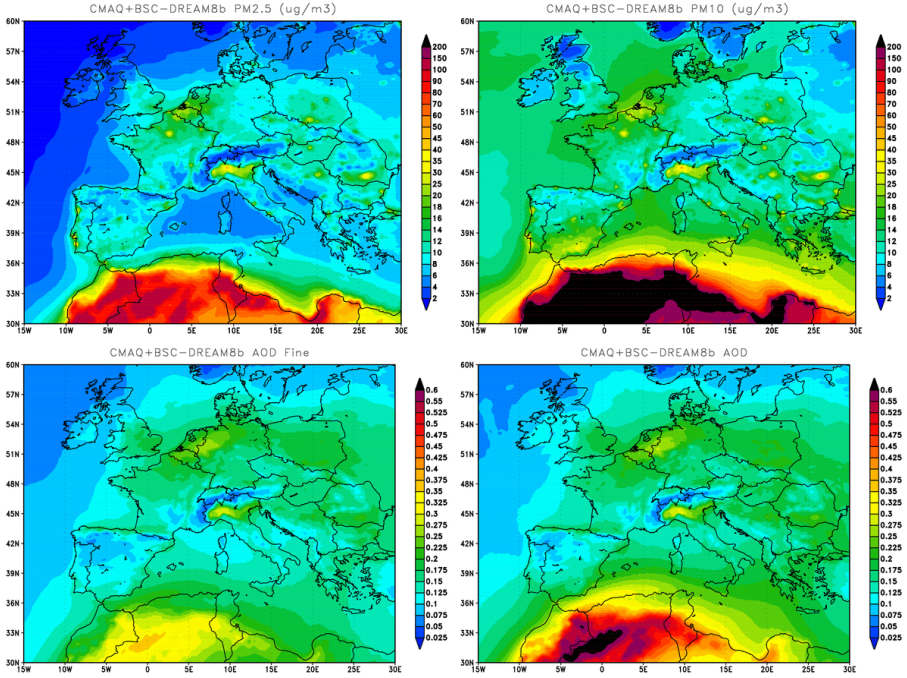

Fig. 8. Annual average of PM2.5 (in $\mu g\,m^{-3}$), PM10 (in $\mu g\,m^{-3}$), AOD_{fine} and AOD obtained with the corrected CMAQ + BSC-DREAM8b simulations. Correction factors of the Table 5 are applied to nitrates, sulphates, ammonium and EC + OC.

ACPD
11, 20575–20629, 2011

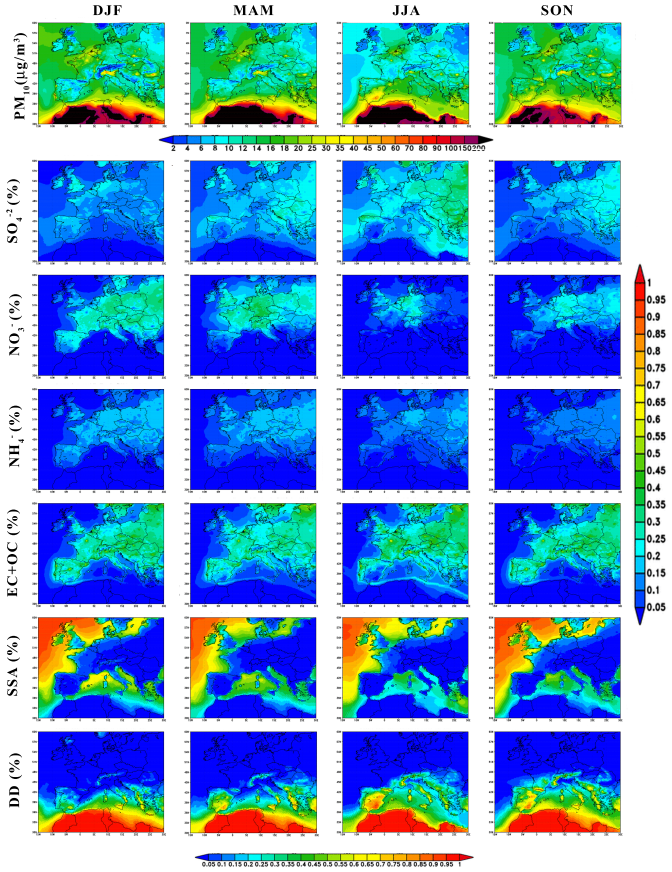

Fig. 9. Seasonal average (from winter to autumn, from left to right panels) of PM10 (in $\mu g\,m^{-3}$) and the seasonal contributions (in %) of sulphates (SO_4^{-2}), nitrates (NO_3^-), ammonium (NH_4^-), carboneous matter (EC + OC), sea salt aerosols (SSA) and desert dust (DD) to PM10 with correction factors of the Table 5 applied to nitrates, sulphates, ammonium and EC + OC.

ACPD
11, 20575–20629, 2011

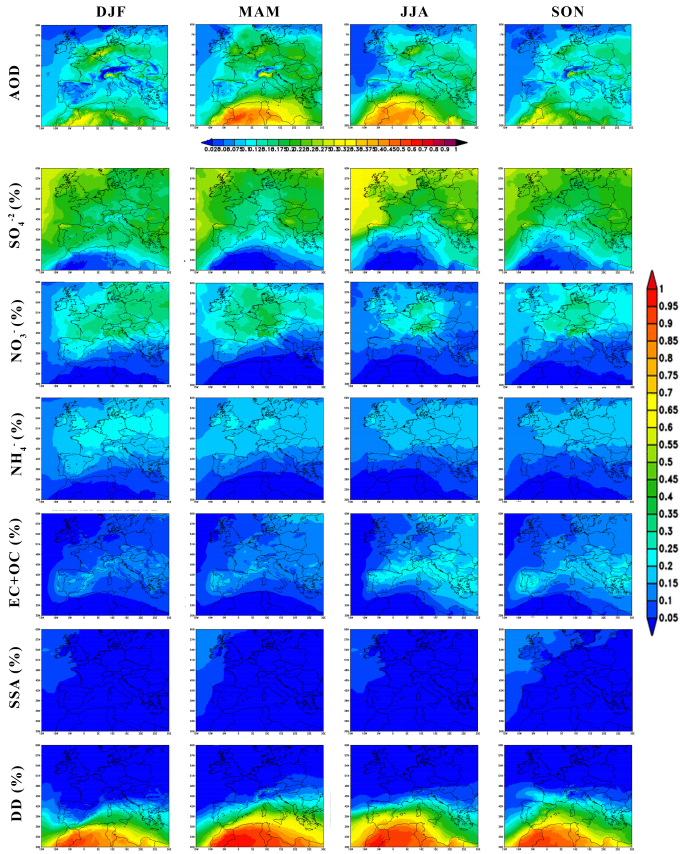

Fig. 10. Seasonal average (from winter to autumn, from left to right panels) of AOD and the seasonal contributions (in %) of sulphates (SO_4^{-2}), nitrates (NO_3^-), ammonium (NH_4^-), carboneous matter (EC + OC), sea salt aerosols (SSA) and desert dust (DD) to AOD with correction factors of the Table 5 applied to nitrates, sulphates, ammonium and EC + OC.

ACPD
11, 20575–20629, 2011

Aerosols in the CALIOPE air quality modelling system

S. Basart et al.

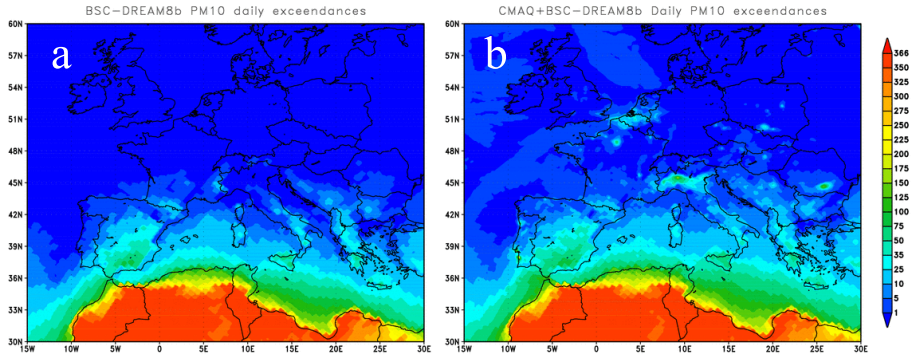

Fig. 11. Number of the days exceeding the EU PM10 daily threshold (>50 µg m^{-3}) for **(a)** BSC-DREAM8b and **(b)** BSC-DREAM8b + CMAQ derived aerosol.

ACPD
11, 20575–20629, 2011